symmetry

MDPI

Article

A Flexible Kernel Regression Decomposition-Based Hybrid Framework for Forecasting Foreign Exchange Rates: Uncovering Symmetric and Asymmetric Market Dynamics

Hasnain Iftikhar [1,*], Said Farooq Shah [1], Fatimah E. Almuhayfith [2,*] and Paulo Canas Rodrigues [3,4]

[1] Department of Statistics, University of Peshawar, Peshawar 25120, Pakistan; farooqshahqau@uop.edu.pk
[2] Department of Mathematics and Statistics, College of Science, King Faisal University, Alahsa 31982, Saudi Arabia
[3] Department of Statistics, Federal University of Bahia, Salvador 40170-110, Brazil; paulo.canas@ufba.br
[4] Department of Business Management, University of Pretoria, Pretoria 0002, South Africa
* Correspondence: hasnain.iftikhar@uop.edu.pk (H.I.); falmuhaifeez@kfu.edu.sa (F.E.A.)

Abstract

Foreign exchange rate forecasting is difficult, as its time series have complex nonlinear and nonstationary dynamics. To this end, the paper proposes a hybrid forecasting framework based on kernel regression decomposition that combines nonparametric trend extraction with linear and nonlinear forecasting models. In the framework we propose, we decompose each series of exchange rates into a long-run trend component and a short-run fluctuation component, which are modeled separately and then combined to generate forecasts. An empirical study based on five major foreign exchange markets shows that the proposed framework consistently outperforms conventional hybrid and standalone forecasting models in multiple forecasting accuracy measures. The statistical validation of the forecasting improvements is confirmed by the Diebold–Mariano test. Moreover, the decomposition offers an interpretable representation of exchange-rate dynamics by distilling persistent long-run movements from localized short-run nonlinear fluctuations. The results indicate that the proposed framework improves forecasting accuracy and offers insight into the structural behavior of foreign exchange markets.

Keywords: symmetry; asymmetry; kernel regression; decomposition-based forecasting; hybrid learning models; nonlinear dependence; exchange-rate dynamics; financial time series

1. Introduction

The foreign exchange (FX) market is the largest and most liquid financial market worldwide. It is critical to international trade and capital flows, portfolio diversification, and global monetary transmission mechanisms [1–4]. However, the exchange rates are important indicators of macroeconomic stability, external competitiveness, inflationary pressures, and financial market expectations [5–7]. The accurate forecasting of exchange rate movements is thus challenging for policymakers, multinational corporations, institutional investors, and financial analysts because of the substantial uncertainty and volatility that characterize global currency markets [8–10]. The prominent currency pairs, such as GBP/USD, EUR/USD, USD/JPY, AUD/USD, and USD/CNY, are the dominant players in the international financial transactions and reserve currency systems [11]. The movements are driven by a complicated interaction between monetary policy decisions, interest rate differentials, geopolitical developments, commodity prices, trade balances, and investor

Check for updates

Academic Editor: Calogero Vetro

Received: 15 July 2026
Revised: 3 August 2026
Accepted: 11 August 2026
Published: 14 August 2026

Copyright: © 2026 by the authors. Licensee MDPI, Basel, Switzerland. This article is an open access article distributed under the terms and conditions of the Creative Commons Attribution (CC BY) license.

sentiment [12]. Moreover, the increase in the level of globalization and financial integration has induced a higher degree of interdependence among currency markets through volatility spillovers, contagion effects, synchronized policy responses, and cross-border capital flows. These features induce nonlinearities, structural breaks, asymmetric adjustments, and time-varying dependencies, which make exchange-rate forecasting particularly challenging for traditional econometric models [13–17].

The FX market plays a central role in the global financial system with an average daily turnover above USD 7.5 trillion, according to the latest Bank for International Settlements (BIS) Triennial Survey [18]. Therefore, accurate exchange rate forecasts are important for portfolio allocation, hedging, derivative pricing, international investment, and monetary policy formulation. However, foreign exchange markets are characterized by a strong nonlinear dependence, volatility clustering, structural breaks, and time-varying dynamics, which seriously limit the performance of conventional linear forecasting models. These challenges motivate the creation of more flexible forecasting frameworks that are able to capture the heterogeneity in exchange-rate dynamics [19].

The last few decades have witnessed a dramatic transformation in time-series forecasting, driven by rapid technological progress, increased computing power, and the growing complexity of financial datasets [20–23]. Stochastic modeling began with Yule's autoregressive (AR) model [24] and continued with Wold's autoregressive moving average (ARMA) representation for stationary processes [25]. Later, Box and Jenkins [26] developed the widely accepted autoregressive integrated moving average (ARIMA) framework, which has become a cornerstone of modern financial econometrics. These models, in turn, motivated the development of volatility extensions, such as generalized autoregressive conditional heteroskedasticity (GARCH), to capture volatility clustering and time-varying volatility observed in financial markets. Traditional linear econometric models are statistically elegant and interpretable, but typically assume stable dependence structures and constant parameters over time. However, empirical evidence indicates that financial time series exhibit nonlinear dynamics, structural instability, regime shifts, asymmetric behavior, and changing stochastic dependence structures, thereby constraining the predictive performance of static linear forecasting methods [27–31]. Recent advances in financial volatility modeling have further extended the capability of parametric time-series models to capture complex market dynamics. For example, periodic bilinear GARCH models, bilinear Markov-switching GARCH models, double-shifted autoregressive Markov models, periodic threshold autorandom volatility models, Markov-switching autorandom volatility models, Markov-switching threshold volatility models, and time-varying asymmetric log GARCH models have demonstrated considerable success in modeling volatility clustering, leverage effects, asymmetric responses, and structural regime changes in financial markets [32–34]. While these models provide valuable insights into conditional volatility dynamics, they are primarily designed to model the evolution of the variance process under specific parametric assumptions. In contrast, the objective of the present study is fundamentally different. Rather than directly modeling conditional volatility, we employ a flexible kernel regression decomposition framework that separates exchange-rate series into smooth long-run trend and irregular short-run fluctuation components before forecasting. This non-parametric decomposition allows the proposed hybrid framework to adapt to heterogeneous symmetric and asymmetric temporal structures, nonlinear dependencies, and non-stationary behavior without imposing restrictive functional forms, thereby providing a flexible forecasting framework for complex foreign exchange markets.

There are still a number of significant research gaps in exchange rate forecasting, despite significant advancements. Exchange rate forecasting is still difficult because of structural instability, volatility clustering, market efficiency, policy interventions, and the

intrinsically nonlinear behavior of financial time series. The robustness and generalizability of existing studies' conclusions are sometimes hampered by their reliance on small datasets, comparatively short sample periods, or unique currency pairs. To overcome these issues, semiparametric, nonparametric, and machine learning-based techniques have been used more frequently in recent studies. Quantile-based methods, including the Conditional Autoregressive Value at Risk (CAViaR) model proposed by Engle and Manganelli [35] and the Exponentially Weighted Quantile Regression (EWQR) model introduced by Taylor [36], have demonstrated superior capability in modeling conditional return distributions, financial risk, and tail behavior [37–41]. Likewise, semiparametric support vector quantile regression, neural networks, support vector machines, tree-based learning algorithms, convolutional neural networks, and hybrid optimization techniques have shown promising forecasting performance for highly nonlinear financial markets [42–46]. Deep learning architectures, such as long short-term memory (LSTM) and gated recurrent unit (GRU) networks, have further improved the modeling of complex temporal dependencies and nonlinear dynamics in exchange rate series [47–49]. However, these approaches are frequently computationally intensive, difficult to understand, prone to overfitting, and may perform erratically in harsh market circumstances. By breaking down time series into several components, decomposition-based forecasting methods like EMD, VMD, STL, and wavelet transforms have improved forecasting accuracy. However, they frequently lack the flexibility to concurrently capture long-term structural trends, short-term stochastic fluctuations, and heterogeneous symmetric and asymmetric temporal dynamics across multiple foreign exchange markets. In order to deliver more accurate and reliable forecasts across a variety of foreign currency markets, a unified kernel regression decomposition-based hybrid forecasting framework that combines the interpretability of econometric models with the flexibility of machine learning is still required [50,51].

Developing reliable statistical forecasting models requires a grasp of the symmetric and asymmetric temporal organization of exchange-rate dynamics in addition to predicting accuracy. Due to varying reactions to macroeconomic news, monetary policy, geopolitical events, and shifts in investor attitude, foreign exchange markets show both symmetric and asymmetric temporal dynamics. Persistent long-term market evolution is a sign of symmetric behavior, while directional market shocks, nonlinear adjustments, and volatility clustering are signs of asymmetric behavior. By using adaptive local smoothing to estimate a smooth trend component and allocating the residual component to the remaining localized nonlinear deviations, the suggested kernel regression decomposition overcomes this difficulty. As a result, the decomposition makes it easier to characterize the exchange-rate series' asymmetric short-run volatility and comparatively symmetric long-run evolution. In this study, asymmetry refers to irregular fluctuations marked by nonlinear responses, volatility clustering, and directional market shocks, as found in the residual component following kernel regression decomposition, while symmetry refers to a consistent, comparatively smooth temporal evolution represented by the trend component. The suggested methodology allows specialized forecasting models to incorporate heterogeneous temporal patterns and enhance forecasting effectiveness by modeling these broken-down components independently. Consequently, this study makes three primary contributions: (i) Exchange-rate series are divided into long-term trend and short-term fluctuation components using a configurable kernel regression decomposition approach. (ii) To describe heterogeneous symmetric and asymmetric temporal dynamics, a unified hybrid forecasting architecture that integrates several kernel functions with both linear (AR, ARIMA) and nonlinear (NPAR, NNAR) forecasting models is suggested. (iii) The superiority, robustness, and generalizability of the suggested methodology over direct hybrid and standalone forecasting methodologies are demonstrated by extensive empirical valida-

tion on five major foreign exchange markets. In contrast to current decomposition-based forecasting techniques, the suggested framework establishes a clear connection between decomposition and temporal market behavior by improving forecasting accuracy while also offering an interpretable statistical representation of relatively symmetric long-run trends and asymmetric short-run market dynamics through kernel regression decomposition. The empirical decomposition analysis also shows that the residual component captures localized heavy-tailed, nonlinear, and asymmetric fluctuations that are then modeled using specialized forecasting models, whereas the estimated trend component explains roughly 95–99% of the total variance across the five exchange-rate series. These results bolster the suggested decomposition strategy's applicability for simulating heterogeneous foreign currency market dynamics and offer empirical evidence for its efficacy.

The remainder of the paper is structured as follows: The proposed hybrid forecasting framework and kernel regression decomposition method are presented in Section 2. The results of the empirical forecasting and the comparative performance analysis are presented in Section 3. Section 4 provides a thorough analysis of the forecasting framework's limitations, applications, and future research directions. The study's main conclusions are finally presented in Section 5.

2. Materials and Methods

In this section, we introduce the proposed kernel regression-based hybrid forecasting framework for modeling nonlinear and nonstationary foreign exchange markets. First, the overall decomposition and forecasting architecture is described. Then, the kernel regression decomposition procedure, forecasting models, parameter estimation strategy and model evaluation methodology are described. Finally, the forecasting experiment, performance measures, and statistical comparison procedures are introduced to comprehensively assess the proposed framework.

2.1. The Proposed Kernel Regression-Based Exchange Rate Forecasting Framework

In this work, we proposes a kernel regression-based decomposition and hybrid forecasting framework for modeling and forecasting major global exchange-rate time series, including GBP/USD, EUR/USD, USD/JPY, AUD/USD, and USD/CNY. These foreign exchange rate series are featured by nonlinear dependence structures, volatility clustering, structural breaks, heavy-tailed distributions, and nonstationary dynamics. Moreover, the dynamics of exchange rate movements often exhibit both symmetric and asymmetric time behavior. Symmetric structures can evolve through repeated cyclical patterns and long-run equilibrium adjustments. Asymmetric dynamics are due to asymmetric responses to positive and negative shocks, volatility clustering and regime-dependent market behavior. Correct modeling of these heterogeneous dynamics is essential for reliable forecasts. But traditional linear models are often unable to capture this complexity, and many machine learning approaches are unable to distinguish long-run trends from short-run fluctuations. The proposed framework addresses this limitation by decomposing each exchange-rate series into long-run trend and short-run fluctuation components using nonparametric kernel regression. Each of these components is modeled independently, and then combined to generate the final forecasts. This provides a flexible and interpretable paradigm for prediction of volatile financial markets.

2.1.1. Kernel Regression-Based Decomposition Technique

In this subsection, we elaborate on the proposed kernel regression-based decomposition technique for forecasting foreign exchange rates. Let $\left\{X_t^{(m)}\right\}_{t=1}^{N}, m \in \{1,2,3,4,5\}$, denote the observed daily foreign exchange rates series, where $m = 1$ for GBP/USD, 2

for EUR/USD, 3 for USD/JPY, 4 for AUD/USD, and 5 for USD/CNY, and N represents the total number of observations. The variable t denotes the time index that corresponds to the chronological order of daily market observations. The observed financial time series is assumed to exhibit both deterministic and stochastic components. Accordingly, the proposed decomposition framework expresses the observed foreign exchange rates as the additive combination of a long-run trend component and a short-run fluctuation component, defined as

$$X_t^{(m)} = L_t^{(m)} + R_t^{(m)}, \qquad t = 1, 2, \ldots, N, \tag{1}$$

where $L_t^{(m)}$ denotes the smooth long-run trend component and $R_t^{(m)}$ represents the short-run fluctuation component. The additive decomposition was chosen because foreign exchange rates are naturally characterized by a smooth long-run trend and short-run stochastic fluctuations. This formulation is particularly suited to nonparametric kernel regression, where the trend is directly estimated and the residual component captures local deviations. Unlike multiplicative decomposition, which is typically appropriate when a series' variability is proportional to its level or exhibits strong seasonal effects, the additive formulation provides a flexible and interpretable representation of exchange-rate dynamics and allows direct reconstruction of the original series. Since the objective of this study is predictive modeling rather than causal inference, no Granger causality analysis was performed between the decomposed components. The trend and fluctuation components are treated as complementary forecasting representations rather than mutually causal processes.

The long-run trend component is estimated using kernel regression smoothing. Kernel regression is a nonparametric estimation technique that estimates the underlying trend structure without imposing any predefined functional relationship between the response and explanatory variables. Kernel regression is better able to model evolving market dynamics and nonlinear temporal structures than parametric trend estimation techniques because it can adapt flexibly to local data characteristics. The following is the kernel regression estimator for the trend component:

$$\widehat{L}_t^{(m)} = \sum_{s=1}^{N} w_{t,s}(h)\, Y_s^{(m)}, \tag{2}$$

where $w_{t,s}(h)$ denotes the normalized kernel weights defined as

$$w_{t,s}(h) = \frac{K\left(\dfrac{t-s}{h}\right)}{\sum_{j=1}^{N} K\left(\dfrac{t-j}{h}\right)}, \tag{3}$$

subject to the normalization condition

$$\sum_{s=1}^{N} w_{t,s}(h) = 1.$$

Equivalently, the trend estimator can be expressed as

$$\widehat{L}_t^{(m)} = \frac{\sum_{s=1}^{N} K\left(\dfrac{t-s}{h}\right) Y_s^{(m)}}{\sum_{s=1}^{N} K\left(\dfrac{t-s}{h}\right)}. \tag{4}$$

The kernel function is denoted by $K(\cdot)$ in the preceding formulation, and the bandwidth parameter, which controls the degree of smoothness, is denoted by $h > 0$. Because it establishes the trade-off between bias and variance, the bandwidth parameter is essential to nonparametric estimation. While bigger bandwidth values yield smoother trend estimates by averaging over wider regions, smaller bandwidth values preserve local fluctuations and nonlinearities by giving greater weight to nearby observations. The choice of bandwidth is crucial for accurately capturing the underlying structures of financial markets. Having obtained the trend component, the fluctuation component will be determined from the residual difference between the observed series and the calculated trend component:

$$\widehat{R}_t^{(m)} = X_t^{(m)} - \widehat{L}_t^{(m)}. \tag{5}$$

The fluctuation component captures high-frequency stochastic information, short-term volatility, irregular market movements, and nonlinear dependencies that are not explained by the long-run trend structure. The adequacy of the decomposition is then assessed by performing distributional analysis of the trend and residual components, variance-explained statistics, and graphical inspection of the decomposed series presented in Section 3.

However, with a theoretical perspective, let $K : \mathbb{R} \to \mathbb{R}$ denote a symmetric kernel function satisfying the standard regularity conditions:

$$\int_{-\infty}^{\infty} K(u)\, du = 1, \tag{6}$$

$$K(u) = K(-u), \tag{7}$$

and

$$\int_{-\infty}^{\infty} u^2 K(u)\, du < \infty. \tag{8}$$

These regularity conditions guarantee that the kernel estimator has desirable statistical properties such as consistency, asymptotic normality, smooth convergence, and stability under mild conditions. Kernel regression smoothing is particularly well suited for financial time series, as it can efficiently capture nonlinear temporal evolution, local structural changes, volatility persistence, and regime-dependent market behavior without requiring strict distributional assumptions. In addition, kernel smoothing is a flexible statistical tool for detecting locally symmetric structures and identifying important asymmetric features in financial data. The resulting decomposition allows the forecasting framework to disentangle persistent regular patterns from asymmetric volatility and shock-driven fluctuations. The kernel function is a crucial factor for the kernel regression performance. Smoothing different kernel architectures is important for the effectiveness of the decomposition. In this work, we use four kernel functions, Gaussian, Epanechnikov, uniform, and truncated Gaussian, to capture different market dynamics and local temporal characteristics, with the Gaussian kernel defined as follows:

$$K(u) = \frac{1}{\sqrt{2\pi}} \exp\left(-\frac{u^2}{2}\right). \tag{9}$$

The Gaussian kernel assigns progressively smaller weights to observations that are further away from the target point. This results in infinitely smooth weighting. This property makes it very useful for assessing persistent financial fluctuations and smooth long-term market structures. The Epanechnikov kernel is given by

$$K(u) = \frac{3}{4}(1 - u^2)\, \mathbb{I}(|u| \leq 1), \tag{10}$$

where $\mathbb{I}(\cdot)$ is the indicator function. The Epanechnikov kernel is a good kernel for local smoothing because it has the best asymptotic efficiency in terms of the mean integrated squared error.

The uniform kernel is defined by

$$K(u) = \frac{1}{2}\mathbb{I}(|u| \leq 1). \tag{11}$$

The uniform kernel, compared to smooth kernels, gives equal weight to all points in the local neighborhood. The simple structure offers stable local averaging properties and computational efficiency.

The truncated Gaussian kernel is given by

$$K(u) = \frac{\phi(u)}{\Phi(a) - \Phi(-a)}\mathbb{I}(|u| \leq a), \tag{12}$$

In the above expression, $a > 0$ is the truncation parameter, and $\phi(\cdot)$ and $\Phi(\cdot)$ are the density and distribution functions of the standard normal distribution, respectively. The truncated Gaussian kernel retains the smooth weighting structure of the Gaussian kernel but provides robustness in volatile markets by reducing the effects of extreme observations and tail events.

In this work, the four kernel functions above were chosen because they represent different classes of local weighting schemes typically used in nonparametric regression. A Uniform kernel is a simple baseline smoother that does not discriminate between observations within the bandwidth. The Gaussian kernel produces weights that are infinitely differentiable and smoothly decreasing with distance and are therefore well suited to capture gradual nonlinear trends. The Epanechnikov kernel is theoretically the optimal kernel for minimum mean integrated squared error (MISE) and provides an efficient trade-off between bias and variance. The truncated Gaussian kernel inherits the smooth weighting property of the Gaussian kernel and has a compact support, which reduces the influence of distant observations while maintaining the local smoothness. These kernels have complementary smoothing properties, and the proposed framework can thus be used to evaluate the robustness of kernel regression decomposition under different local weighting mechanisms. The four kernels were chosen to represent the main types of kernel weighting functions: discontinuous (uniform), compact-support optimal (Epanechnikov), globally smooth (Gaussian), and compactly supported smooth (truncated Gaussian). This choice facilitates a comprehensive evaluation of kernel regression decomposition for exchange-rate forecasting.

To further compare the proposed decomposition framework with existing decomposition methods commonly used in financial time-series forecasting, Table 1 presents a summary of the main methodological characteristics of these methods. Different from EMD, VMD, STL, and wavelet-based decomposition, kernel regression estimates the underlying trend directly by adaptive local smoothing without the necessity of iterative mode extraction, predefined basis functions, or frequency band selection. These properties make kernel regression especially attractive for building interpretable, decomposition-based hybrid forecasting models for nonlinear and nonstationary foreign exchange time series.

2.1.2. Modeling the Decomposed Components

In this subsection, the kernel regression decomposition of the trend and the fluctuation components are modeled separately with linear and nonlinear forecasting models. This component-wise strategy of the proposed framework can better capture the heterogeneous temporal structures than directly modeling the original exchange rate series. Thus, a

specialized forecasting model can be assigned for each component, leading to better prediction performance and interpretability. To this end, each component is modeled with the following four forecasting techniques.

Table 1. A methodological comparison of representative and kernel regression decomposition for financial time series forecasting.

Feature	EMD	VMD	STL	Wavelet	Kernel Regression
Nonparametric	✓	✓	✓	×	✓
Adaptive local smoothing	×	×	Limited	×	✓
Need pre-defined basis functions	×	×	×	✓	×
Frequency domain decomposition	×	✓	×	✓	×
Iterative decomposition	✓	✓	×	✓	×
Resistance to mode mixing	Low	High	High	High	High
Sensitivity analysis	High	Moderate	Low	Moderate	Low
Direct estimation of smooth trends	Limited	Moderate	✓	Limited	✓
Suitable for non-stationary, non-linear data	✓	✓	Moderate	✓	✓
No frequency band selection needed	✓	×	✓	×	✓
Simple hybrid forecasting integration	Moderate	Moderate	High	Moderate	High
Interpretability of components of decomposition	Moderate	Moderate	High	Moderate	High

Autoregressive Model

In the time-series forecasting models, one of the most basic linear stochastic forecasting models is the autoregressive model. It is predicated on the idea that the present observation is linearly dependent on its prior values [52]. For a component that is stationary

$$X_t^{(m)} \in \{L_t^{(m)}, R_t^{(m)}\},$$

the AR(p) process is defined as

$$X_t^{(m)} = \sum_{i=1}^{p} \phi_i X_{t-i}^{(m)} + \varepsilon_t^{(m)}, \tag{13}$$

where $\varepsilon_t^{(m)}$ represents a white-noise process with zero mean and constant variance, and ϕ_i are autoregressive coefficients. When simulating smooth temporal persistence and short-memory linear dependence in financial time series, the AR model excels.

Autoregressive Moving Average Model

By adding moving-average variables that capture shock propagation and serial dependence in the innovation process, the ARMA model extends the AR framework [53]. The expression for the ARMA(p, q) model is

$$X_t^{(m)} = \sum_{i=1}^{p} \phi_i X_{t-i}^{(m)} + \varepsilon_t^{(m)} + \sum_{j=1}^{q} \theta_j \varepsilon_{t-j}^{(m)}, \tag{14}$$

where ϕ_i and θ_j denote the autoregressive and moving-average parameters, respectively. The ARMA model simultaneously captures persistence and shock-transmission dynamics, thereby providing greater flexibility in modeling financial market behavior.

Nonparametric Autoregressive Model

Financial time series frequently exhibit nonlinear temporal dependence that cannot be adequately captured by linear models, despite their computational efficiency and statistical interpretability [54]. The Nonparametric Autoregressive (NPAR) model is used to overcome

this restriction. By explicitly predicting unknown nonlinear functions from the data, the NPAR model loosens linearity assumptions. The definition of the NPAR model is

$$X_t^{(m)} = \sum_{i=1}^{p} f_i\left(X_{t-i}^{(m)}\right) + \varepsilon_t^{(m)}, \qquad X_t^{(m)} \in \left\{L_t^{(m)}, R_t^{(m)}\right\}. \tag{15}$$

where $f_i(\cdot)$ are smooth unknown nonlinear functions estimated nonparametrically. The NPAR framework is highly flexible and can capture nonlinear dependence structures, asymmetric market behavior, and local stochastic variations.

Neural Network Autoregressive Model

To further improve nonlinear forecasting capability, the Neural Network Autoregressive (NNAR) model is incorporated into the proposed framework. The NNAR model serves as a universal function approximator, capable of learning highly complex nonlinear relationships directly from historical observations [55]. For a component $X_t^{(m)}$, the NNAR(p, k) model is defined as

$$X_t^{(m)} = \alpha_0 + \sum_{j=1}^{k} \alpha_j g\left(\beta_{j0} + \sum_{i=1}^{p} \beta_{ji} X_{t-i}^{(m)}\right) + \varepsilon_t^{(m)}, \tag{16}$$

where $g(\cdot)$ denotes a nonlinear activation function, k represents the number of hidden neurons, and α_j and β_{ji} are neural network parameters. The NNAR model effectively captures nonlinear interactions, volatility clustering, threshold effects, and higher-order temporal dependencies commonly observed in financial markets.

2.1.3. Model Parameter Selection

To ensure consistency, reproducibility, and objective model specification, all forecasting models were estimated using automatic data-driven parameter selection procedures. During the expanding-window forecasting experiment, model parameters were re-estimated at each forecasting origin using only the information available up to that time, thereby preventing look-ahead bias and ensuring a fair out-of-sample comparison among all competing forecasting models. Table 2 summarizes the software packages, parameter selection procedures, and implementation settings adopted throughout the forecasting framework.

For the linear forecasting models, the autoregressive order of the AR model and the (p, d, q) orders of the ARIMA model were selected automatically using the Akaike Information Criterion (AIC), with the differencing order determined simultaneously within the automatic model selection procedure. The nonlinear autoregressive neural network (NNAR) models were implemented using the `nnar()` function from the `forecast` package [56] in `R`, where the autoregressive lag order was selected automatically and the number of hidden neurons was determined according to the default rule $k = \left\lfloor \frac{p+1}{2} \right\rfloor$, where p denotes the selected autoregressive lag order. The nonparametric autoregressive (NPAR) models were estimated using the `aar()` function from the `tsDyn` package [57]. Following the empirical specification adopted in this study, the embedding dimension was fixed at $m = 3$ for the trend component and $m = 2$ for the residual component.

For the proposed kernel regression decomposition, the smoothing bandwidth was estimated automatically using the least-squares cross-validation (LSCV) criterion implemented in the `np` package [58]. The LSCV method finds the optimal bandwidth by minimizing the cross-validation prediction error and therefore provides a good compromise between under- and over-smoothing without the need for subjective tuning of parameters. The Gaussian, Epanechnikov, uniform, and truncated Gaussian kernels are implemented using

the default specifications provided by the `np` package, with the truncated Gaussian kernel using the default second-order implementation for all empirical analysis.

Table 2. Summary of software packages, parameter selection procedures, and implementation settings used in the forecasting framework.

Component	Software/Package	Parameter Selection	Implementation Setting
AR	`forecast`	Lag order selected using AIC	Re-estimated at each expanding window
ARIMA	`forecast`	Orders (p, d, q) selected using AIC	Re-estimated at each expanding window
NPAR	`tsDyn`	Automatic local autoregressive estimation	Embedding dimension: $m = 3$ (trend), $m = 2$ (residual)
NNAR	`forecast`	Automatic lag selection; hidden neurons determined by $k = \lfloor (p+1)/2 \rfloor$	Re-estimated at each expanding window
Kernel bandwidth	`np`	Least-squares cross-validation (LSCV)	Re-estimated at each expanding window
Gaussian kernel	`np`	Default implementation	Standard Gaussian kernel
Epanechnikov kernel	`np`	Default implementation	Standard Epanechnikov kernel
Uniform kernel	`np`	Default implementation	Standard uniform kernel
Truncated Gaussian kernel	`np`	Default implementation	Second-order truncated Gaussian kernel

To evaluate the robustness of the proposed decomposition framework with respect to bandwidth selection, an additional bandwidth sensitivity analysis was performed by re-estimating the complete forecasting framework using bandwidths around the LSCV-selected optimum. The corresponding empirical results are presented and discussed in Section 4.

In this work, a uniform notation system is introduced for all hybrid kernel regression-based forecasting models to provide a more systematic, comprehensible, and scalable representation of the proposed forecasting structures. Each hybrid forecasting model is uniquely identified by three elements: (i) the kernel function used for decomposition, (ii) the forecasting model assigned to the trend component, and (iii) the forecasting model assigned to the fluctuation component. For example, the notation ${}^{G}\mathbb{H}^{IA}$ represents a hybrid forecasting structure in which the Gaussian kernel decomposition method is employed, the trend component is modeled using the ARIMA model, and the fluctuation component is modeled using the AR model. Similarly, ${}^{U}\mathbb{H}^{DD}$ denotes a uniform kernel decomposition framework in which both the trend and fluctuation components are modeled with NNAR models. Using this generalized representation, the total number of hybrid forecasting structures developed in this study can be formally expressed as $4(\text{kernels}) \times 4^2(16 \text{ combinatoin of forecating models}) = 64$. Therefore, the proposed notation system provides a mathematically rigorous, scalable, and interpretable representation of the complete kernel regression-based hybrid forecasting framework, facilitating systematic comparison and performance evaluation across all proposed forecasting architectures.

2.2. Expanding-Window One-Step-Ahead Forecasting Procedure

The forecasting experiments were conducted using an expanding-window forecasting framework. Let t denote the forecasting origin. At each iteration, only observations available up to time t were used for kernel decomposition, model estimation, and forecast generation. A one-step-ahead forecast for time $(t + 1)$ was then produced. Then the newly observed value was added to the estimation sample, and the procedure was then repeated sequentially until the end of the evaluation period. Thus, no information prior to the forecasting horizon is used in the decomposition and forecasting steps, respectively, eliminating the possibility of look-ahead bias/information leakage. The empirical analysis

uses daily foreign exchange time-series data spanning January 2016 to December 2025. Daily data from 2016–2022 were used for model estimation, and 2023–2025 for out-of-sample forecasting. Forecasts are generated recursively under the expanding-window framework throughout the testing period.

2.3. Performance Evaluation Metrics

In this work, we employ various statistical measures of accuracy and efficiency to evaluate the forecasting performance in detail. The mathematical formulas for the following measures: Mean Absolute Error (MAE), Root Mean Square Error (RMSE), Mean Absolute Percentage Error (MAPE), Correlation Coefficient (CORR), Directional Accuracy (DA), Nash–Sutcliffe Efficiency (NSE), and Kling–Gupta Efficiency (KGE) are listed in Table 3.

Table 3. Forecast evaluation metrics employed for performance assessment.

Metric	Mathematical Expression
MAE	$\frac{1}{N}\sum_{t=1}^{N}\left\lvert X_t^{(m)} - \widehat{X}_t^{(m)}\right\rvert$
RMSE	$\sqrt{\frac{1}{N}\sum_{t=1}^{N}\left(X_t^{(m)} - \widehat{X}_t^{(m)}\right)^2}$
MAPE	$\frac{100}{N}\sum_{t=1}^{N}\left\lvert\frac{X_t^{(m)} - \widehat{X}_t^{(m)}}{X_t^{(m)}}\right\rvert$
CORR	$\frac{\sum_{t=1}^{N}\left(X_t^{(m)} - \bar{X}^{(m)}\right)\left(\widehat{X}_t^{(m)} - \bar{\widehat{X}}^{(m)}\right)}{\sqrt{\sum_{t=1}^{N}\left(X_t^{(m)} - \bar{X}^{(m)}\right)^2}\sqrt{\sum_{t=1}^{N}\left(\widehat{X}_t^{(m)} - \bar{\widehat{X}}^{(m)}\right)^2}}$
DA	$\frac{1}{N-1}\sum_{t=2}^{N}\mathbb{I}\left[\left(X_t^{(m)} - X_{t-1}^{(m)}\right)\left(\widehat{X}_t^{(m)} - \widehat{X}_{t-1}^{(m)}\right) > 0\right]$
NSE	$1 - \frac{\sum_{t=1}^{N}\left(X_t^{(m)} - \widehat{X}_t^{(m)}\right)^2}{\sum_{t=1}^{N}\left(X_t^{(m)} - \bar{X}^{(m)}\right)^2}$
KGE	$1 - \sqrt{(r-1)^2 + \left(\frac{\mu_s}{\mu_o} - 1\right)^2 + \left(\frac{\sigma_s}{\sigma_o} - 1\right)^2}$

Collectively, these evaluation metrics provide a statistically comprehensive framework for assessing forecasting accuracy, predictive stability, directional consistency, and model robustness across multiple FX markets.

In addition to the above, to further assess the statistical significance of the forecasting improvements achieved by the proposed kernel regression-based hybrid framework, the Diebold–Mariano (DM) test [59] was employed. Unlike conventional error measures such as MAPE, MAE, and RMSE, which quantify forecasting accuracy, the DM test evaluates whether the predictive performance of two competing forecasting models differs significantly. Let $e_{1,t}$ and $e_{2,t}$ denote the forecast errors generated by two competing forecasting models at time t. Based on a specified loss function $L(\cdot)$, the loss differential is defined as $d_t = L(e_{1,t}) - L(e_{2,t})$, $t = 1, 2, \ldots, T$, where T denotes the total number of out-of-sample forecasts. In this study, the squared-error loss function, $L(e_t) = e_t^2$, was adopted. The null hypothesis states that the proposed model does not outperform the benchmark, whereas the alternative hypothesis indicates that the proposed model has a lower expected forecast loss. Specifically, $H_0 : E(d_t) \geq 0$, against the one-sided alternative, $H_1 : E(d_t) < 0$; rejection of the null hypothesis indicates that the proposed forecasting model achieves significantly superior predictive accuracy compared with the competing model. The DM test statistic is computed as $DM = \frac{\bar{d}}{\sqrt{\widehat{\mathrm{Var}}(\bar{d})}}$, where $\bar{d} = \frac{1}{T}\sum_{t=1}^{T} d_t$ is the sample mean of the loss differential, and $\widehat{\mathrm{Var}}(\bar{d})$ denotes a consistent estimate of its variance that accounts for possible serial correlation in the forecast loss differentials. In this study, the DM test was employed to compare the proposed kernel regression-based hybrid forecasting models

with the best-performing direct hybrid and standalone forecasting models for each foreign exchange market.

Table 4 summarizes the relative computational characteristics of the forecasting models considered in this study. Linear models such as AR and ARIMA exhibit low computational requirements and high interpretability due to their simple parametric structures. In contrast, NPAR and NNAR models are computationally more demanding because they involve nonparametric smoothing procedures and iterative optimization algorithms. Nevertheless, within the proposed kernel regression decomposition framework, the forecasting models are applied to statistically simpler, decomposed subseries rather than to the original exchange-rate series, thereby reducing effective modeling complexity and improving computational efficiency. The decomposition step makes the underlying symmetric and asymmetric temporal structures simpler by separating smooth trend components from irregular fluctuations. This makes it possible for later forecasting models to learn each component more effectively. For realistic financial forecasting applications, the significant increases in forecasting accuracy outweigh the longer training times required by NNAR-based hybrid models.

Table 4. Qualitative comparison of computational complexity and training characteristics of the forecasting models.

Model	Model Type	Approximate Complexity	Training Time	Interpretability
AR	Linear	$\mathcal{O}(Np^2)$	Very Low	High
ARIMA	Linear	$\mathcal{O}(N(p+q)^2)$	Low	High
NPAR	Nonparametric	$\mathcal{O}(N^2)$	Moderate	Moderate
NNAR	Nonlinear	$\mathcal{O}(NEpk)$	High	Low

Notation: N denotes the number of observations; p is the autoregressive order; q is the moving-average order; k is the number of hidden neurons in the NNAR model; and E denotes the number of training epochs.

Figure 1 shows the general structure of the proposed forecasting framework, which includes kernel regression decomposition, hybrid component modeling, forecast reconstruction, and statistical performance evaluation.

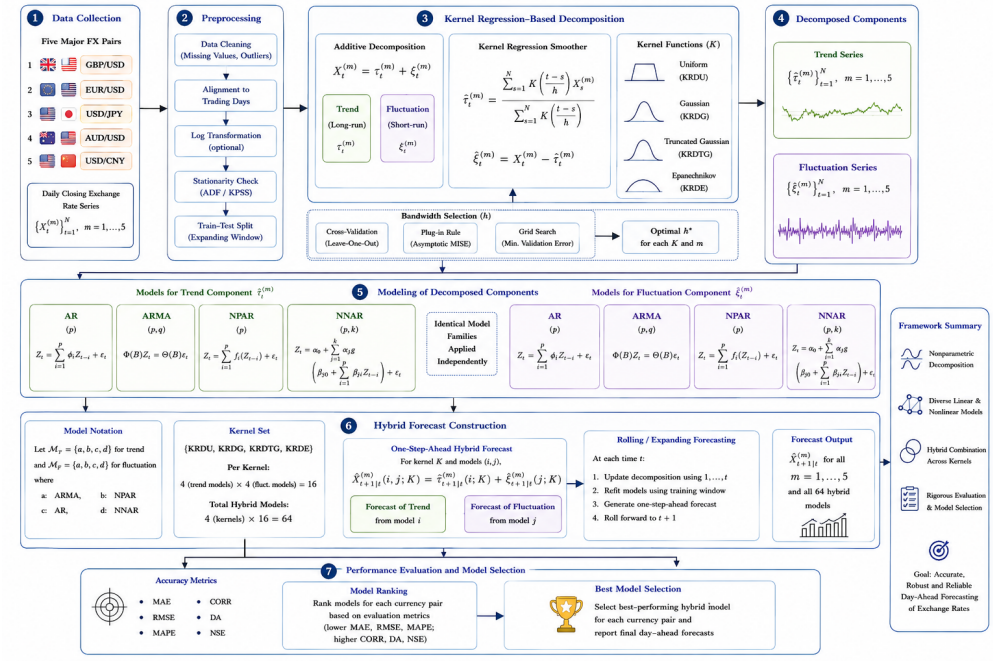


Figure 1. A complete flowchart of the proposed forecasting framework.

3. Results

In this paper, we propose a kernel regression-based decomposition framework to produce day-ahead forecasts of major foreign exchange rates, using the financial time series of the major currency markets, namely, GBP/USD, EUR/USD, USD/JPY, AUD/USD, and USD/CNY. The downloaded exchange-rate datasets were checked for missing values and data consistency prior to analysis. There were no missing observations, and no imputation procedures were needed. Furthermore, we did not delete any outliers, as extreme changes in the exchange rate are real market behavior and are required to assess forecasting models under realistic financial conditions. The data are from Yahoo Finance, and they include daily data for 10 years, from January 2016 to December 2025, for the major economies, which represent a large portion of global forex trading. For the forecasting experiment, we used a strict chronological train–test split to avoid data leakage. The first seven years of observations (January 2016–December 2022) were dedicated only to kernel regression decomposition, bandwidth selection, model estimation and parameter tuning, whereas the last three years (January 2023–December 2025) were dedicated only to out-of-sample evaluation. Trend and fluctuation components were estimated using only the training data, and forecasting models were fitted to the decomposed training series. The forecasts for the testing period were generated sequentially without using any future observations, which provided an unbiased evaluation of the proposed hybrid forecasting framework.

However, a visual analysis is shown in Figure 2, which confirmed that these exchange rates are highly nonlinear and nonstationary with long-term trends, structural changes, and volatility clustering. The currency pairs in question are strange in their own ways. GBP/USD and EUR/USD are medium-term cyclical amid macroeconomic uncertainties and shifts in monetary policy in their respective regions. The USD/JPY pair is characterized by large regime shifts and asymmetric volatility driven by global risk sentiment and the diverging monetary policies of Japan and the United States. AUD/USD is heavily influenced by commodity price movements and external demand, while USD/CNY is characterized by slow structural changes caused by currency regulation and geopolitical factors. Moreover, generalized volatility and sharp exchange rate movements are the most pronounced during the periods of global financial distress, inflationary episodes, post-pandemic recovery and periods of differential monetary policies. The results stress the need for a proposed forecasting framework that can accurately handle both long-term trends and short-term stochastic fluctuations in exchange-rate dynamics.

In this paper, the terms *symmetric* and *asymmetric* are used mainly to define the time evolution of the decomposed components, and not the probability distributions. The trend component is assumed to be relatively symmetric because it captures smooth, persistent long-run movements that change gradually over time, without sudden changes in direction. In contrast, the residual component is considered asymmetric because it concentrates on localized market shocks, volatility clustering, and nonlinear adjustments that occur irregularly over time. Distributional statistics such as skewness and kurtosis are reported only to support this temporal interpretation rather than to define symmetry in a purely probabilistic sense.

However, Figure 3 shows the kernel regression decomposition for the EUR/USD exchange rate. In each subfigure, the upper panel shows the original series of exchange rates and the estimated kernel trend component. The kernel trend closely follows the long-run movement of the exchange rate and effectively smooths short-run fluctuations. The estimated trend is stable even in the face of large market movements, such as during the COVID-19 pandemic and the subsequent changes in monetary policy, and it reflects the underlying structural behavior without over-smoothing or introducing artificial oscillations. It implies that the proposed kernel regression method can uncover the persistent component

of the exchange rate while preserving the overall market dynamics. However, the middle panel shows the residual component after removing the estimated trend. The residual series oscillates around zero for the whole period of the sample and does not show any systematic long-run drift. This shows that the decomposition manages to separate persistent market behavior from irregular short-term fluctuations. There are a few times where we see temporary spikes in volatility, especially in times of market uncertainty, but these are still centered around zero, and so they are asymmetric deviations in the short run rather than changes in the underlying equilibrium trend. This behavior supports the interpretation that the kernel regression decomposition effectively isolates transient nonlinear market shocks. Finally, the lower panel reports the empirical distribution of the residual component. The residuals are centered around zero and are roughly symmetric. The heavier tails indicate the presence of occasional large market shocks commonly observed in financial time series. This result is consistent with the statistical evidence reported in Table 5, where the trend component explains 95% to 99% of the total variance of the exchange rates, while the residual component is characterized by higher kurtosis and significant conditional heteroscedasticity. These results jointly indicate that the proposed decomposition preserves the economically meaningful long-run information in the trend, while the nonlinear and asymmetric short-run dynamics are concentrated in the residual component, thus providing a suitable representation for the subsequent hybrid forecasting setup.

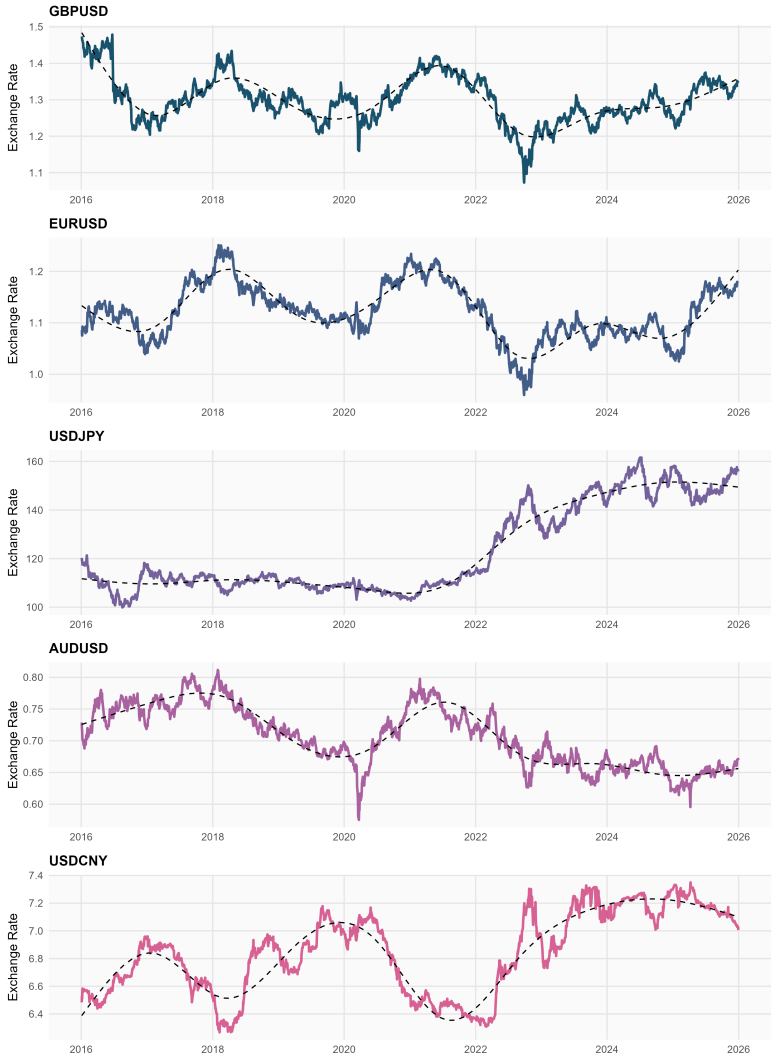


Figure 2. Time-series plot for all considered markets.

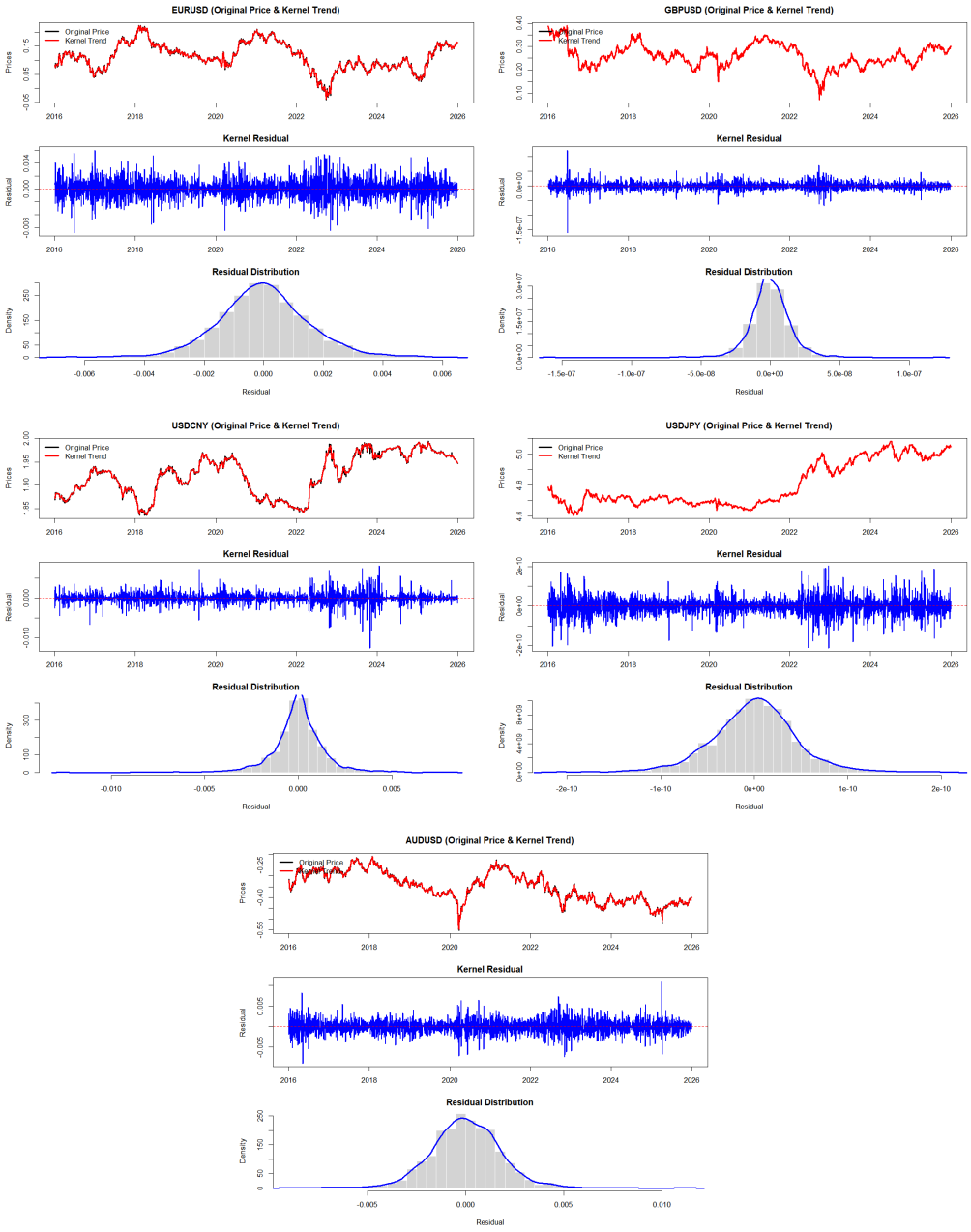


Figure 3. Decomposition of kernel regression across five foreign exchange markets. Each panel displays the original exchange rate, the estimated kernel trend (**top**), the extracted residual component (**middle**), and the empirical distribution of the residuals (**bottom**).

Besides the above graphical analysis, Table 5 reports the distributional properties of the trend and residual components obtained from the proposed kernel regression decomposition for the five foreign exchange markets. We find that the decomposition successfully separates the persistent long-run market dynamics from the high-frequency short-run fluctuations while preserving the fundamental statistical properties of each component. The trend component accounts for a very substantial part of the total variance of all exchange rates, between 95.1% and 98.7% of the observed variance. It implies that the kernel regression captures well the major long-run movements of the exchange rates with a fairly small share of the variability assigned to the residual component. This is also supported by the standard deviations, where the residual components have a substantially smaller dispersion than the corresponding trend components. The trend component accounts for between 95.1% and 98.7% of the total variance across the five exchange-rate series, indicating that

kernel regression successfully captures the dominant long-run evolution of the exchange rates. However, a high explained variance should not be interpreted as implying that the residual component is unimportant for forecasting. Rather, the residual contains localized nonlinear fluctuations, volatility clustering, and short-term market shocks that cannot be explained by the smooth trend. Its variance is relatively small but it contains important predictive information about short-run exchange-rate dynamics. Therefore, the proposed hybrid framework models the trend and residual components separately, allowing linear models to capture the persistent long-run structure, while nonlinear models are used to model the complex residual behavior. Therefore, the improved forecasting performance in the empirical analysis is due to the additional information contained in both components and not only in the trend component.

Table 5. Distributional properties of the components of the kernel regression decomposition.

Series	Trend Component				Residual Component				Variance Explained (%)
	SD	Skewness	Kurtosis	ARCH *p*-Value	SD	Skewness	Kurtosis	ARCH *p*-Value	
GBP/USD	0.054	0.140	3.112	<0.001	0.013	−0.407	16.403	<0.001	95.4
EUR/USD	0.048	0.034	2.665	<0.001	0.010	0.019	4.074	<0.001	95.8
USD/JPY	17.950	0.061	2.779	<0.001	2.340	0.007	5.795	<0.001	98.3
AUD/USD	0.049	0.050	2.434	<0.001	0.011	0.007	4.736	<0.001	95.1
USD/CNY	0.298	−0.188	1.826	<0.001	0.034	−0.490	11.265	<0.001	98.7

The distributional measures provide additional evidence supporting the characteristics of the decomposed components. The trend components exhibit relatively small skewness values, ranging from −0.188 to 0.140, indicating that the extracted long-run movements are approximately symmetric from a distributional perspective with only minor departures from normality. Their kurtosis values are also close to or below three for most exchange-rate series, suggesting that the long-run dynamics evolve smoothly after high-frequency fluctuations have been removed. In contrast, the residual components display substantially larger kurtosis values, particularly for GBP/USD (16.403) and USD/CNY (11.265), indicating pronounced heavy-tailed behavior and the presence of occasional extreme short-run market movements. Although the residual skewness remains moderate, the relatively larger values observed for GBP/USD (−0.407) and USD/CNY (−0.490) suggest that short-run market responses are more asymmetric than the corresponding long-run trends. The proposed interpretation of the decomposition is also supported by the distributional statistics. The small skewness of trend components is consistent with the roughly symmetric long-run movements revealed by the kernel regression framework, while the higher kurtosis and marginally higher skewness of residual components are indicative of heavy-tailed short-run market shocks. These distributional features are not the only interpretation, and the terms *symmetric* and *asymmetric* are in this study more a description of the temporal development of the exchange-rate series than of their statistical distributions.

On the other hand, the ARCH LM test further confirms the distinct statistical characteristics of the decomposed components. For every exchange-rate series, the null hypothesis of homoskedasticity is strongly rejected ($p < 0.001$), indicating the presence of persistent conditional heteroskedasticity. While both the trend and residual components exhibit ARCH effects, the volatility associated with the residual component primarily reflects localized short-run market shocks after the smooth long-run trend has been removed. The significant ARCH effects observed in the residual components indicate persistent volatility clustering, whereby periods of high volatility tend to be followed by periods of high volatility and periods of low volatility tend to be followed by periods of low volatility. This represents a well-established stylized fact of financial time series and should not be interpreted as a

limitation of the proposed decomposition framework. Instead, it demonstrates that the kernel regression decomposition successfully extracts the smooth long-run market evolution while preserving the economically meaningful time-varying volatility within the residual component. Consequently, the residual component retains valuable predictive information that justifies its separate modeling using nonlinear forecasting models within the proposed hybrid forecasting framework. Overall, the empirical evidence demonstrates that the proposed kernel regression decomposition effectively separates the exchange-rate series into two statistically and economically meaningful components. The trend component captures the relatively smooth and persistent long-run market evolution, whereas the residual component concentrates localized nonlinear shocks, volatility clustering, and heavy-tailed behavior associated with short-run market dynamics. Therefore, throughout this study, the terms *symmetric* and *asymmetric* refer primarily to the temporal evolution of the decomposed components, while the reported skewness and kurtosis statistics provide complementary distributional evidence supporting this interpretation. These findings further justify modeling the trend and residual components separately within the proposed hybrid forecasting framework.

The decomposition results in Figure 3 and Table 5 show that the proposed kernel regression framework successfully decomposes each exchange-rate series into statistically distinct long-run trend (L_t) and short-run fluctuation (R_t) components. The decomposition is performed for four kernel specifications, namely, the uniform (${}^{U}\mathbb{H}$), Gaussian (${}^{G}\mathbb{H}$), truncated Gaussian (${}^{TG}\mathbb{H}$), and Epanechnikov (${}^{E}\mathbb{H}$). Then, the extracted trend and fluctuation components are further modeled with linear (AR and ARIMA) and nonlinear (NPAR and NNAR) forecasting models separately, which provide a complete set of hybrid forecasting structures. The forecasting performance of these models across the five foreign exchange markets for each kernel specification is considered. Tables 6–10 report the one-step-ahead forecasting results for GBP/USD, EUR/USD, USD/JPY, AUD/USD, and USD/CNY, respectively.

However, the best-three forecasting models for GBP/USD exchange rate are ${}^{E}\mathbb{H}^{ID}$, ${}^{E}\mathbb{H}^{DD}$, and ${}^{U}\mathbb{H}^{ID}$ (see Table 6). Among these, ${}^{E}\mathbb{H}^{ID}$ has the best performance with 0.08490 MAPE, 0.00090 MAE, 0.00120 RMSE, 0.99940 CORR, 0.99870 NSE, 0.99580 KGE, and 0.89660 DA. The second-best model, ${}^{E}\mathbb{H}^{DD}$, performs very well with MAPE = 0.08950, RMSE = 0.00130, CORR = 0.99930, and NSE = 0.99860, which proves that the fully NNAR-based forecasting frameworks are still very powerful when using the Epanechnikov kernel decomposition. The uniform kernel-based model is denoted as ${}^{U}\mathbb{H}^{ID}$, which achieves superior performance metrics: MAPE = 0.10640, RMSE = 0.00160, CORR = 0.99910, NSE = 0.99800, KGE = 0.99420. The results show that adaptive kernel smoothing with nonlinear forecasting models can significantly improve the predictive accuracy of GBP/USD forecasting.

For the EUR/USD exchange rate (Table 7), the best-three forecasting models are ${}^{E}\mathbb{H}^{ID}$, ${}^{TG}\mathbb{H}^{ID}$, and ${}^{U}\mathbb{H}^{ID}$. The overall best model, ${}^{E}\mathbb{H}^{ID}$, exhibits very high forecasting accuracy with MAPE = 0.12920, MAE = 0.00137, RMSE = 0.00187, CORR = 0.99920, NSE = 0.99830, KGE = 0.99610, and DA = 0.79800. The truncated Gaussian model ${}^{TG}\mathbb{H}^{ID}$ has the second-best performance with MAPE = 0.17010, RMSE = 0.00258, CORR = 0.99840, and NSE = 0.99660, indicating good stability and predictive consistency. The uniform kernel-based model ${}^{U}\mathbb{H}^{ID}$ also performs comparably with MAPE = 0.16110, RMSE = 0.00238, CORR = 0.99870, and NSE = 0.99720. The results confirm that hybrid structures with ARIMA and NNAR forecasting components outperform in forecasting EUR/USD dynamics.

Table 6. The out-of-sample one-step-ahead forecasting accuracy of all sixty-four hybrid models for GBP/USD using the proposed forecasting framework.

S.No	Model	MAPE	MAE	RMSE	CORR	DA	NSE	KGE
1	${}^{G}\mathbb{H}^{AA}$	0.36840	0.00480	0.00630	0.98550	0.50000	0.97110	0.98540
2	${}^{G}\mathbb{H}^{AI}$	0.36870	0.00490	0.00640	0.98540	0.49750	0.97090	0.98510
3	${}^{G}\mathbb{H}^{AN}$	0.36790	0.00470	0.00620	0.98570	0.50250	0.97130	0.98580
4	${}^{G}\mathbb{H}^{AD}$	0.36740	0.00460	0.00610	0.98590	0.50500	0.97150	0.98620
5	${}^{G}\mathbb{H}^{IA}$	0.36840	0.00480	0.00630	0.98550	0.50000	0.97110	0.98540
6	${}^{G}\mathbb{H}^{II}$	0.36880	0.00490	0.00640	0.98540	0.49750	0.97080	0.98500
7	${}^{G}\mathbb{H}^{IN}$	0.36780	0.00470	0.00620	0.98570	0.50250	0.97130	0.98590
8	${}^{G}\mathbb{H}^{ID}$	0.36720	0.00460	0.00610	0.98590	0.50500	0.97160	0.98630
9	${}^{G}\mathbb{H}^{NA}$	0.37060	0.00480	0.00630	0.98540	0.50000	0.97080	0.98280
10	${}^{G}\mathbb{H}^{NI}$	0.37090	0.00490	0.00640	0.98530	0.49750	0.97060	0.98250
11	${}^{G}\mathbb{H}^{NN}$	0.37010	0.00470	0.00620	0.98560	0.50250	0.97100	0.98320
12	${}^{G}\mathbb{H}^{ND}$	0.36960	0.00460	0.00610	0.98580	0.50500	0.97120	0.98360
13	${}^{G}\mathbb{H}^{DA}$	0.36910	0.00480	0.00630	0.98550	0.50000	0.97090	0.98540
14	${}^{G}\mathbb{H}^{DI}$	0.36940	0.00490	0.00640	0.98540	0.49750	0.97070	0.98510
15	${}^{G}\mathbb{H}^{DN}$	0.36860	0.00470	0.00620	0.98570	0.50250	0.97110	0.98580
16	${}^{G}\mathbb{H}^{DD}$	0.36810	0.00460	0.00610	0.98590	0.50500	0.97130	0.98620
17	${}^{E}\mathbb{H}^{AA}$	0.12040	0.00160	0.00200	0.99860	0.84240	0.99710	0.99360
18	${}^{E}\mathbb{H}^{AI}$	0.12070	0.00170	0.00210	0.99850	0.83990	0.99700	0.99330
19	${}^{E}\mathbb{H}^{AN}$	0.11980	0.00150	0.00190	0.99870	0.84730	0.99720	0.99400
20	${}^{E}\mathbb{H}^{AD}$	0.11890	0.00140	0.00180	0.99880	0.84980	0.99740	0.99440
21	${}^{E}\mathbb{H}^{IA}$	0.08620	0.00110	0.00140	0.99920	0.88920	0.99850	0.99500
22	${}^{E}\mathbb{H}^{II}$	0.08650	0.00120	0.00150	0.99910	0.88670	0.99840	0.99470
23	${}^{E}\mathbb{H}^{IN}$	0.08570	0.00100	0.00130	0.99930	0.89410	0.99860	0.99540
24	${}^{E}\mathbb{H}^{ID}$	0.08490	0.00090	0.00120	0.99940	0.89660	0.99870	0.99580
25	${}^{E}\mathbb{H}^{NA}$	0.14490	0.00190	0.00240	0.99790	0.80300	0.99560	0.99170
26	${}^{E}\mathbb{H}^{NI}$	0.14530	0.00200	0.00250	0.99780	0.80050	0.99540	0.99140
27	${}^{E}\mathbb{H}^{NN}$	0.14380	0.00180	0.00230	0.99800	0.80790	0.99580	0.99210
28	${}^{E}\mathbb{H}^{ND}$	0.14260	0.00170	0.00220	0.99810	0.81030	0.99600	0.99250
29	${}^{E}\mathbb{H}^{DA}$	0.14130	0.00180	0.00240	0.99790	0.79560	0.99590	0.99230
30	${}^{E}\mathbb{H}^{DI}$	0.14170	0.00190	0.00250	0.99780	0.79310	0.99570	0.99200
31	${}^{E}\mathbb{H}^{DN}$	0.14050	0.00170	0.00230	0.99800	0.80050	0.99600	0.99270
32	${}^{E}\mathbb{H}^{DD}$	0.13940	0.00160	0.00220	0.99820	0.80300	0.99620	0.99310
33	${}^{U}\mathbb{H}^{AA}$	0.12150	0.00160	0.00200	0.99860	0.82270	0.99710	0.99310
34	${}^{U}\mathbb{H}^{AI}$	0.12180	0.00170	0.00210	0.99850	0.82020	0.99700	0.99280
35	${}^{U}\mathbb{H}^{AN}$	0.12090	0.00150	0.00190	0.99870	0.82760	0.99720	0.99350
36	${}^{U}\mathbb{H}^{AD}$	0.12010	0.00140	0.00180	0.99880	0.83000	0.99740	0.99390
37	${}^{U}\mathbb{H}^{IA}$	0.10770	0.00140	0.00180	0.99890	0.85220	0.99770	0.99340
38	${}^{U}\mathbb{H}^{II}$	0.10800	0.00150	0.00190	0.99880	0.84980	0.99760	0.99310
39	${}^{U}\mathbb{H}^{IN}$	0.10710	0.00130	0.00170	0.99900	0.85710	0.99780	0.99380
40	${}^{U}\mathbb{H}^{ID}$	0.10640	0.00120	0.00160	0.99910	0.85960	0.99800	0.99420
41	${}^{U}\mathbb{H}^{NA}$	0.12140	0.00160	0.00200	0.99860	0.82760	0.99710	0.99090
42	${}^{U}\mathbb{H}^{NI}$	0.12170	0.00170	0.00210	0.99850	0.82510	0.99700	0.99060
43	${}^{U}\mathbb{H}^{NN}$	0.12070	0.00150	0.00190	0.99870	0.83000	0.99720	0.99130
44	${}^{U}\mathbb{H}^{ND}$	0.11990	0.00140	0.00180	0.99880	0.83250	0.99740	0.99170
45	${}^{U}\mathbb{H}^{DA}$	0.12000	0.00160	0.00200	0.99860	0.81530	0.99720	0.99170
46	${}^{U}\mathbb{H}^{DI}$	0.12030	0.00170	0.00210	0.99850	0.81280	0.99710	0.99140
47	${}^{U}\mathbb{H}^{DN}$	0.11910	0.00150	0.00190	0.99870	0.81770	0.99730	0.99210
48	${}^{U}\mathbb{H}^{DD}$	0.11820	0.00140	0.00180	0.99880	0.82020	0.99750	0.99250
49	${}^{TG}\mathbb{H}^{AA}$	0.28510	0.00370	0.00490	0.99130	0.62560	0.98270	0.98840
50	${}^{TG}\mathbb{H}^{AI}$	0.28550	0.00380	0.00500	0.99120	0.62320	0.98250	0.98810
51	${}^{TG}\mathbb{H}^{AN}$	0.28430	0.00360	0.00480	0.99150	0.62810	0.98290	0.98880
52	${}^{TG}\mathbb{H}^{AD}$	0.28340	0.00350	0.00470	0.99170	0.63050	0.98310	0.98920
53	${}^{TG}\mathbb{H}^{IA}$	0.26630	0.00350	0.00450	0.99250	0.61330	0.98500	0.99120
54	${}^{TG}\mathbb{H}^{II}$	0.26670	0.00360	0.00460	0.99240	0.61080	0.98480	0.99090
55	${}^{TG}\mathbb{H}^{IN}$	0.26520	0.00340	0.00440	0.99260	0.61820	0.98520	0.99160

Table 6. *Cont.*

S.No	Model	MAPE	MAE	RMSE	CORR	DA	NSE	KGE
56	${}^{TG}\mathbb{H}^{ID}$	0.26400	0.00330	0.00430	0.99280	0.62070	0.98550	0.99200
57	${}^{TG}\mathbb{H}^{NA}$	0.28590	0.00370	0.00490	0.99130	0.62560	0.98260	0.98650
58	${}^{TG}\mathbb{H}^{NI}$	0.28630	0.00380	0.00500	0.99120	0.62320	0.98240	0.98620
59	${}^{TG}\mathbb{H}^{NN}$	0.28500	0.00360	0.00480	0.99150	0.62810	0.98280	0.98690
60	${}^{TG}\mathbb{H}^{ND}$	0.28410	0.00350	0.00470	0.99170	0.63050	0.98300	0.98730
61	${}^{TG}\mathbb{H}^{DA}$	0.28470	0.00370	0.00480	0.99140	0.62560	0.98280	0.99010
62	${}^{TG}\mathbb{H}^{DI}$	0.28510	0.00380	0.00490	0.99130	0.62320	0.98260	0.98980
63	${}^{TG}\mathbb{H}^{DN}$	0.28390	0.00360	0.00470	0.99160	0.62810	0.98300	0.99050
64	${}^{TG}\mathbb{H}^{DD}$	0.28300	0.00350	0.00460	0.99180	0.63050	0.98320	0.99100

Table 7. The out-of-sample one-step-ahead forecasting accuracy of all sixty-four hybrid models for the EUR/USD employing the proposed forecasting framework.

S.No	Model	MAPE	MAE	RMSE	CORR	DA	NSE	KGE
1	${}^{G}\mathbb{H}^{AA}$	0.20310	0.00221	0.00311	0.99760	0.68720	0.99510	0.99500
2	${}^{G}\mathbb{H}^{AI}$	0.20300	0.00220	0.00310	0.99760	0.68720	0.99520	0.99510
3	${}^{G}\mathbb{H}^{AN}$	0.20280	0.00220	0.00309	0.99770	0.68960	0.99520	0.99510
4	${}^{G}\mathbb{H}^{AD}$	0.20240	0.00219	0.00308	0.99770	0.69210	0.99530	0.99520
5	${}^{G}\mathbb{H}^{IA}$	0.19890	0.00218	0.00301	0.99770	0.68960	0.99530	0.99540
6	${}^{G}\mathbb{H}^{II}$	0.19870	0.00217	0.00300	0.99770	0.69210	0.99540	0.99550
7	${}^{G}\mathbb{H}^{IN}$	0.19860	0.00217	0.00299	0.99770	0.69460	0.99540	0.99550
8	${}^{G}\mathbb{H}^{ID}$	0.19830	0.00216	0.00298	0.99780	0.69700	0.99550	0.99560
9	${}^{G}\mathbb{H}^{NA}$	0.21610	0.00241	0.00322	0.99730	0.68230	0.99460	0.99340
10	${}^{G}\mathbb{H}^{NI}$	0.21590	0.00240	0.00320	0.99730	0.68470	0.99470	0.99350
11	${}^{G}\mathbb{H}^{NN}$	0.21570	0.00239	0.00319	0.99740	0.68720	0.99470	0.99350
12	${}^{G}\mathbb{H}^{ND}$	0.21550	0.00238	0.00318	0.99740	0.68960	0.99480	0.99360
13	${}^{G}\mathbb{H}^{DA}$	0.21640	0.00242	0.00323	0.99730	0.68230	0.99450	0.99420
14	${}^{G}\mathbb{H}^{DI}$	0.21620	0.00241	0.00322	0.99730	0.68470	0.99460	0.99430
15	${}^{G}\mathbb{H}^{DN}$	0.21600	0.00240	0.00321	0.99740	0.68720	0.99470	0.99430
16	${}^{G}\mathbb{H}^{DD}$	0.21580	0.00239	0.00319	0.99740	0.68960	0.99470	0.99440
17	${}^{E}\mathbb{H}^{AA}$	0.13100	0.00141	0.00191	0.99910	0.79310	0.99810	0.99570
18	${}^{E}\mathbb{H}^{AI}$	0.13080	0.00140	0.00190	0.99910	0.79560	0.99820	0.99580
19	${}^{E}\mathbb{H}^{AN}$	0.13060	0.00139	0.00189	0.99920	0.79800	0.99820	0.99580
20	${}^{E}\mathbb{H}^{AD}$	0.13040	0.00138	0.00188	0.99920	0.80050	0.99830	0.99590
21	${}^{E}\mathbb{H}^{IA}$	0.12990	0.00140	0.00190	0.99910	0.79060	0.99810	0.99590
22	${}^{E}\mathbb{H}^{II}$	0.12970	0.00139	0.00189	0.99910	0.79310	0.99820	0.99600
23	${}^{E}\mathbb{H}^{IN}$	0.12950	0.00138	0.00188	0.99920	0.79560	0.99820	0.99600
24	${}^{E}\mathbb{H}^{ID}$	0.12920	0.00137	0.00187	0.99920	0.79800	0.99830	0.99610
25	${}^{E}\mathbb{H}^{NA}$	0.15660	0.00171	0.00231	0.99860	0.79310	0.99720	0.99480
26	${}^{E}\mathbb{H}^{NI}$	0.15640	0.00170	0.00230	0.99860	0.79560	0.99730	0.99490
27	${}^{E}\mathbb{H}^{NN}$	0.15630	0.00169	0.00229	0.99860	0.79800	0.99730	0.99490
28	${}^{E}\mathbb{H}^{ND}$	0.15610	0.00168	0.00228	0.99870	0.80050	0.99740	0.99500
29	${}^{E}\mathbb{H}^{DA}$	0.15640	0.00171	0.00231	0.99860	0.79310	0.99720	0.99560
30	${}^{E}\mathbb{H}^{DI}$	0.15620	0.00170	0.00230	0.99860	0.79560	0.99730	0.99570
31	${}^{E}\mathbb{H}^{DN}$	0.15610	0.00169	0.00229	0.99870	0.79800	0.99730	0.99570
32	${}^{E}\mathbb{H}^{DD}$	0.15590	0.00168	0.00228	0.99870	0.80050	0.99740	0.99580
33	${}^{U}\mathbb{H}^{AA}$	0.16410	0.00181	0.00241	0.99850	0.74380	0.99690	0.99660
34	${}^{U}\mathbb{H}^{AI}$	0.16390	0.00180	0.00240	0.99850	0.74630	0.99700	0.99670
35	${}^{U}\mathbb{H}^{AN}$	0.16370	0.00179	0.00239	0.99850	0.74880	0.99700	0.99670
36	${}^{U}\mathbb{H}^{AD}$	0.16350	0.00178	0.00238	0.99860	0.75120	0.99710	0.99680
37	${}^{U}\mathbb{H}^{IA}$	0.16170	0.00181	0.00241	0.99850	0.74880	0.99700	0.99600
38	${}^{U}\mathbb{H}^{II}$	0.16150	0.00180	0.00240	0.99860	0.75120	0.99710	0.99610
39	${}^{U}\mathbb{H}^{IN}$	0.16130	0.00179	0.00239	0.99860	0.75370	0.99710	0.99610
40	${}^{U}\mathbb{H}^{ID}$	0.16110	0.00178	0.00238	0.99860	0.75620	0.99720	0.99620
41	${}^{U}\mathbb{H}^{NA}$	0.16820	0.00191	0.00251	0.99840	0.75370	0.99670	0.99470

Table 7. *Cont.*

S.No	Model	MAPE	MAE	RMSE	CORR	DA	NSE	KGE
42	${}^{U}\mathbb{H}^{NI}$	0.16800	0.00190	0.00250	0.99840	0.75620	0.99680	0.99480
43	${}^{U}\mathbb{H}^{NN}$	0.16780	0.00189	0.00249	0.99850	0.75860	0.99680	0.99480
44	${}^{U}\mathbb{H}^{ND}$	0.16760	0.00188	0.00248	0.99850	0.76110	0.99690	0.99490
45	${}^{U}\mathbb{H}^{DA}$	0.16760	0.00181	0.00251	0.99840	0.75620	0.99680	0.99550
46	${}^{U}\mathbb{H}^{DI}$	0.16740	0.00180	0.00250	0.99840	0.75860	0.99690	0.99560
47	${}^{U}\mathbb{H}^{DN}$	0.16720	0.00179	0.00249	0.99850	0.76110	0.99690	0.99560
48	${}^{U}\mathbb{H}^{DD}$	0.16700	0.00178	0.00248	0.99850	0.76350	0.99700	0.99570
49	${}^{TG}\mathbb{H}^{AA}$	0.18090	0.00201	0.00271	0.99810	0.72910	0.99610	0.99510
50	${}^{TG}\mathbb{H}^{AI}$	0.18070	0.00200	0.00270	0.99810	0.73150	0.99620	0.99520
51	${}^{TG}\mathbb{H}^{AN}$	0.18050	0.00199	0.00269	0.99820	0.73400	0.99620	0.99520
52	${}^{TG}\mathbb{H}^{AD}$	0.18020	0.00198	0.00268	0.99820	0.73650	0.99630	0.99530
53	${}^{TG}\mathbb{H}^{IA}$	0.17070	0.00191	0.00261	0.99820	0.74630	0.99640	0.99570
54	${}^{TG}\mathbb{H}^{II}$	0.17050	0.00190	0.00260	0.99830	0.74880	0.99650	0.99580
55	${}^{TG}\mathbb{H}^{IN}$	0.17030	0.00189	0.00259	0.99830	0.75120	0.99650	0.99580
56	${}^{TG}\mathbb{H}^{ID}$	0.17010	0.00188	0.00258	0.99840	0.75370	0.99660	0.99590
57	${}^{TG}\mathbb{H}^{NA}$	0.19990	0.00221	0.00301	0.99770	0.70690	0.99530	0.99390
58	${}^{TG}\mathbb{H}^{NI}$	0.19970	0.00220	0.00300	0.99770	0.70940	0.99540	0.99400
59	${}^{TG}\mathbb{H}^{NN}$	0.19950	0.00219	0.00299	0.99770	0.71180	0.99540	0.99400
60	${}^{TG}\mathbb{H}^{ND}$	0.19930	0.00218	0.00298	0.99780	0.71430	0.99550	0.99410
61	${}^{TG}\mathbb{H}^{DA}$	0.20020	0.00221	0.00301	0.99770	0.70440	0.99530	0.99470
62	${}^{TG}\mathbb{H}^{DI}$	0.20000	0.00220	0.00300	0.99770	0.70690	0.99540	0.99480
63	${}^{TG}\mathbb{H}^{DN}$	0.19980	0.00219	0.00299	0.99770	0.70940	0.99540	0.99480
64	${}^{TG}\mathbb{H}^{DD}$	0.19960	0.00218	0.00298	0.99780	0.71180	0.99550	0.99490

Table 8. The out-of-sample one-step-ahead forecasting accuracy of all sixty-four hybrid models for USD/JPY using the proposed forecasting framework.

S.No	Model	MAPE	MAE	RMSE	CORR	DA	NSE	KGE
1	${}^{G}\mathbb{H}^{AA}$	0.51680	0.77590	1.02110	0.97610	0.50490	0.95200	0.97590
2	${}^{G}\mathbb{H}^{AI}$	0.51660	0.77570	1.02090	0.97610	0.50740	0.95210	0.97600
3	${}^{G}\mathbb{H}^{AN}$	0.51640	0.77550	1.02070	0.97620	0.50990	0.95220	0.97610
4	${}^{G}\mathbb{H}^{AD}$	0.51610	0.77510	1.02030	0.97620	0.51230	0.95230	0.97620
5	${}^{G}\mathbb{H}^{IA}$	0.51600	0.77500	1.02010	0.97630	0.51480	0.95240	0.97630
6	${}^{G}\mathbb{H}^{II}$	0.51580	0.77480	1.01990	0.97630	0.51720	0.95250	0.97640
7	${}^{G}\mathbb{H}^{IN}$	0.51560	0.77450	1.01970	0.97640	0.51970	0.95260	0.97650
8	${}^{G}\mathbb{H}^{ID}$	0.51530	0.77420	1.01940	0.97640	0.52220	0.95270	0.97660
9	${}^{G}\mathbb{H}^{NA}$	0.51850	0.77840	1.02290	0.97590	0.50250	0.95170	0.97570
10	${}^{G}\mathbb{H}^{NI}$	0.51830	0.77820	1.02260	0.97600	0.50490	0.95180	0.97580
11	${}^{G}\mathbb{H}^{NN}$	0.51810	0.77790	1.02240	0.97600	0.50740	0.95190	0.97590
12	${}^{G}\mathbb{H}^{ND}$	0.51780	0.77760	1.02200	0.97610	0.50990	0.95200	0.97600
13	${}^{G}\mathbb{H}^{DA}$	0.55870	0.84080	1.07900	0.97360	0.50490	0.94640	0.95560
14	${}^{G}\mathbb{H}^{DI}$	0.55840	0.84040	1.07860	0.97370	0.50740	0.94650	0.95570
15	${}^{G}\mathbb{H}^{DN}$	0.55810	0.84000	1.07820	0.97380	0.50990	0.94660	0.95580
16	${}^{G}\mathbb{H}^{DD}$	0.55780	0.83960	1.07780	0.97390	0.51230	0.94670	0.95590
17	${}^{E}\mathbb{H}^{AA}$	0.18620	0.27950	0.35930	0.99700	0.80790	0.99400	0.99210
18	${}^{E}\mathbb{H}^{AI}$	0.18590	0.27910	0.35890	0.99700	0.81030	0.99410	0.99220
19	${}^{E}\mathbb{H}^{AN}$	0.18530	0.27820	0.35820	0.99710	0.81530	0.99420	0.99230
20	${}^{E}\mathbb{H}^{AD}$	0.18510	0.27790	0.35790	0.99710	0.81770	0.99430	0.99240
21	${}^{E}\mathbb{H}^{IA}$	0.17550	0.26350	0.33950	0.99730	0.81530	0.99460	0.99320
22	${}^{E}\mathbb{H}^{II}$	0.17520	0.26310	0.33900	0.99740	0.81770	0.99470	0.99330
23	${}^{E}\mathbb{H}^{IN}$	0.17480	0.26240	0.33820	0.99750	0.82020	0.99480	0.99340
24	${}^{E}\mathbb{H}^{ID}$	0.17460	0.26210	0.33790	0.99750	0.82270	0.99490	0.99350
25	${}^{E}\mathbb{H}^{NA}$	0.23420	0.35170	0.45420	0.99520	0.78330	0.99040	0.99330
26	${}^{E}\mathbb{H}^{NI}$	0.23400	0.35140	0.45380	0.99530	0.78570	0.99050	0.99350
27	${}^{E}\mathbb{H}^{NN}$	0.23370	0.35100	0.45290	0.99540	0.78820	0.99060	0.99360

Table 8. *Cont.*

S.No	Model	MAPE	MAE	RMSE	CORR	DA	NSE	KGE
28	${}^{E}\mathbb{H}^{ND}$	0.23350	0.35070	0.45250	0.99540	0.79060	0.99070	0.99370
29	${}^{E}\mathbb{H}^{DA}$	0.24630	0.37040	0.47290	0.99480	0.77830	0.98960	0.98720
30	${}^{E}\mathbb{H}^{DI}$	0.24600	0.37000	0.47240	0.99490	0.78080	0.98970	0.98740
31	${}^{E}\mathbb{H}^{DN}$	0.24570	0.36950	0.47180	0.99500	0.78330	0.98980	0.98750
32	${}^{E}\mathbb{H}^{DD}$	0.24540	0.36910	0.47120	0.99500	0.78570	0.98990	0.98760
33	${}^{U}\mathbb{H}^{AA}$	0.22790	0.34200	0.45100	0.99520	0.77090	0.99050	0.99360
34	${}^{U}\mathbb{H}^{AI}$	0.22760	0.34160	0.45050	0.99530	0.77340	0.99060	0.99370
35	${}^{U}\mathbb{H}^{AN}$	0.22720	0.34100	0.44890	0.99540	0.77590	0.99070	0.99380
36	${}^{U}\mathbb{H}^{AD}$	0.22690	0.34060	0.44830	0.99550	0.77830	0.99080	0.99390
37	${}^{U}\mathbb{H}^{IA}$	0.22490	0.33760	0.44520	0.99530	0.76850	0.99080	0.99310
38	${}^{U}\mathbb{H}^{II}$	0.22460	0.33720	0.44470	0.99540	0.77090	0.99090	0.99320
39	${}^{U}\mathbb{H}^{IN}$	0.22420	0.33660	0.44320	0.99550	0.77340	0.99100	0.99330
40	${}^{U}\mathbb{H}^{ID}$	0.22390	0.33620	0.44270	0.99560	0.77590	0.99110	0.99340
41	${}^{U}\mathbb{H}^{NA}$	0.23790	0.35710	0.46630	0.99490	0.76850	0.98990	0.99250
42	${}^{U}\mathbb{H}^{NI}$	0.23750	0.35650	0.46570	0.99500	0.77090	0.99000	0.99260
43	${}^{U}\mathbb{H}^{NN}$	0.23690	0.35570	0.46440	0.99510	0.77340	0.99010	0.99270
44	${}^{U}\mathbb{H}^{ND}$	0.23660	0.35520	0.46380	0.99510	0.77590	0.99020	0.99280
45	${}^{U}\mathbb{H}^{DA}$	0.24800	0.37300	0.49070	0.99440	0.76600	0.98880	0.98560
46	${}^{U}\mathbb{H}^{DI}$	0.24770	0.37250	0.49010	0.99450	0.76850	0.98890	0.98580
47	${}^{U}\mathbb{H}^{DN}$	0.24740	0.37200	0.48930	0.99460	0.77090	0.98900	0.98590
48	${}^{U}\mathbb{H}^{DD}$	0.24710	0.37150	0.48870	0.99470	0.77340	0.98910	0.98600
49	${}^{TG}\mathbb{H}^{AA}$	0.43280	0.64980	0.85050	0.98320	0.56900	0.96660	0.98240
50	${}^{TG}\mathbb{H}^{AI}$	0.43250	0.64940	0.85000	0.98330	0.57140	0.96670	0.98250
51	${}^{TG}\mathbb{H}^{AN}$	0.43220	0.64900	0.84960	0.98340	0.57390	0.96680	0.98260
52	${}^{TG}\mathbb{H}^{AD}$	0.43190	0.64850	0.84910	0.98350	0.57640	0.96690	0.98270
53	${}^{TG}\mathbb{H}^{IA}$	0.41910	0.62920	0.83050	0.98400	0.57390	0.96810	0.98390
54	${}^{TG}\mathbb{H}^{II}$	0.41880	0.62880	0.83000	0.98410	0.57640	0.96820	0.98400
55	${}^{TG}\mathbb{H}^{IN}$	0.41850	0.62840	0.82960	0.98420	0.57880	0.96830	0.98410
56	${}^{TG}\mathbb{H}^{ID}$	0.41820	0.62800	0.82910	0.98430	0.58130	0.96840	0.98420
57	${}^{TG}\mathbb{H}^{NA}$	0.43300	0.65000	0.85200	0.98310	0.56900	0.96650	0.98180
58	${}^{TG}\mathbb{H}^{NI}$	0.43270	0.64960	0.85150	0.98320	0.57140	0.96660	0.98190
59	${}^{TG}\mathbb{H}^{NN}$	0.43240	0.64920	0.85110	0.98330	0.57390	0.96670	0.98200
60	${}^{TG}\mathbb{H}^{ND}$	0.43210	0.64870	0.85060	0.98340	0.57640	0.96680	0.98210
61	${}^{TG}\mathbb{H}^{DA}$	0.48150	0.72480	0.92850	0.98070	0.54680	0.96020	0.95250
62	${}^{TG}\mathbb{H}^{DI}$	0.48110	0.72430	0.92800	0.98080	0.54930	0.96030	0.95260
63	${}^{TG}\mathbb{H}^{DN}$	0.48080	0.72380	0.92760	0.98090	0.55170	0.96040	0.95280
64	${}^{TG}\mathbb{H}^{DD}$	0.48050	0.72330	0.92710	0.98100	0.55420	0.96050	0.95290

While ${}^{E}\mathbb{H}^{ID}$, ${}^{U}\mathbb{H}^{ID}$, and ${}^{TG}\mathbb{H}^{ID}$ are the three best forecast models for the USD/JPY exchange rate (Table 8). The best model is ${}^{E}\mathbb{H}^{ID}$ (MAPE = 0.1746, MAE = 0.2621, RMSE = 0.3379, CORR = 0.9975, NSE = 0.9949, KGE = 0.9935, and DA = 0.8227). The second-best model is the uniform kernel model ${}^{U}\mathbb{H}^{ID}$ with MAPE = 0.2239, RMSE = 0.4427, CORR = 0.9956, and NSE = 0.9911. Even applying simple smoothing techniques, this model has very good predictive power. The truncated Gaussian model ${}^{TG}\mathbb{H}^{ID}$ takes third place with MAPE = 0.4182, RMSE = 0.8291, CORR = 0.9843, and NSE = 0.9684. The results show that adaptive local smoothing, in conjunction with nonlinear forecasting models, significantly enhances predictive accuracy in volatile USD/JPY markets.

On the other hand, the best models for the AUD/USD exchange rate (Table 9) are ${}^{U}\mathbb{H}^{DD}$, ${}^{E}\mathbb{H}^{ID}$, and ${}^{TG}\mathbb{H}^{ID}$. The best forecasting performance is obtained by the uniform kernel-based model ${}^{U}\mathbb{H}^{DD}$ with MAPE = 0.1519, MAE = 0.0009, RMSE = 0.0013, CORR = 0.9964, NSE = 0.9925, KGE = 0.9886, and DA = 0.8522. The Epanechnikov kernel model ${}^{E}\mathbb{H}^{ID}$ is close, with MAPE = 0.0978, RMSE = 0.0013, CORR = 0.9987, NSE = 0.9973 and DA = 0.8966, which shows better performance in directional forecasting. The truncated Gaussian specification ${}^{TG}\mathbb{H}^{ID}$ also records MAPE = 0.2157, RMSE = 0.0018, CORR = 0.9926,

and NSE = 0.9851. These results show that the nonlinear structure of NNAR-based forecasting always improves the forecasting accuracy for AUD/USD compared with alternative kernel decomposition approaches.

Table 9. The out-of-sample one-step-ahead forecasting accuracy of all sixty-four hybrid models for the AUD/USD employing the proposed forecasting framework.

S.No	Model	MAPE	MAE	RMSE	CORR	DA	NSE	KGE
1	${}^{G}\mathbb{H}^{AA}$	0.26090	0.00170	0.00230	0.98870	0.64780	0.97750	0.98550
2	${}^{G}\mathbb{H}^{AI}$	0.26110	0.00170	0.00230	0.98860	0.64530	0.97740	0.98520
3	${}^{G}\mathbb{H}^{AN}$	0.26040	0.00170	0.00220	0.98890	0.65020	0.97780	0.98610
4	${}^{G}\mathbb{H}^{AD}$	0.26010	0.00170	0.00220	0.98900	0.65270	0.97790	0.98650
5	${}^{G}\mathbb{H}^{IA}$	0.25780	0.00170	0.00230	0.98890	0.63790	0.97790	0.98650
6	${}^{G}\mathbb{H}^{II}$	0.25800	0.00170	0.00230	0.98880	0.63550	0.97780	0.98620
7	${}^{G}\mathbb{H}^{IN}$	0.25740	0.00170	0.00220	0.98910	0.64290	0.97810	0.98710
8	${}^{G}\mathbb{H}^{ID}$	0.25710	0.00160	0.00220	0.98920	0.64530	0.97830	0.98750
9	${}^{G}\mathbb{H}^{NA}$	0.26190	0.00170	0.00230	0.98840	0.67000	0.97670	0.98010
10	${}^{G}\mathbb{H}^{NI}$	0.26210	0.00170	0.00230	0.98830	0.66750	0.97650	0.97980
11	${}^{G}\mathbb{H}^{NN}$	0.26150	0.00170	0.00220	0.98860	0.67240	0.97700	0.98090
12	${}^{G}\mathbb{H}^{ND}$	0.26120	0.00170	0.00220	0.98870	0.67490	0.97720	0.98150
13	${}^{G}\mathbb{H}^{DA}$	0.26240	0.00170	0.00230	0.98840	0.67000	0.97680	0.98240
14	${}^{G}\mathbb{H}^{DI}$	0.26260	0.00170	0.00230	0.98830	0.66750	0.97660	0.98210
15	${}^{G}\mathbb{H}^{DN}$	0.26200	0.00170	0.00220	0.98860	0.67240	0.97700	0.98310
16	${}^{G}\mathbb{H}^{DD}$	0.26180	0.00160	0.00220	0.98870	0.67490	0.97720	0.98360
17	${}^{E}\mathbb{H}^{AA}$	0.16400	0.00110	0.00140	0.99570	0.79560	0.99140	0.98820
18	${}^{E}\mathbb{H}^{AI}$	0.16420	0.00110	0.00140	0.99560	0.79310	0.99130	0.98790
19	${}^{E}\mathbb{H}^{AN}$	0.16350	0.00110	0.00130	0.99590	0.79800	0.99160	0.98910
20	${}^{E}\mathbb{H}^{AD}$	0.16290	0.00100	0.00130	0.99600	0.80050	0.99180	0.98980
21	${}^{E}\mathbb{H}^{IA}$	0.09870	0.00110	0.00140	0.99850	0.89160	0.99700	0.99110
22	${}^{E}\mathbb{H}^{II}$	0.09890	0.00110	0.00140	0.99840	0.88920	0.99680	0.99080
23	${}^{E}\mathbb{H}^{IN}$	0.09820	0.00100	0.00130	0.99860	0.89410	0.99710	0.99210
24	${}^{E}\mathbb{H}^{ID}$	0.09780	0.00100	0.00130	0.99870	0.89660	0.99730	0.99280
25	${}^{E}\mathbb{H}^{NA}$	0.18280	0.00120	0.00160	0.99440	0.81280	0.98860	0.98270
26	${}^{E}\mathbb{H}^{NI}$	0.18300	0.00120	0.00160	0.99430	0.81030	0.98840	0.98240
27	${}^{E}\mathbb{H}^{NN}$	0.18110	0.00120	0.00150	0.99460	0.81770	0.98890	0.98380
28	${}^{E}\mathbb{H}^{ND}$	0.18070	0.00110	0.00150	0.99470	0.82020	0.98910	0.98450
29	${}^{E}\mathbb{H}^{DA}$	0.18050	0.00120	0.00160	0.99450	0.81530	0.98880	0.98600
30	${}^{E}\mathbb{H}^{DI}$	0.18080	0.00120	0.00160	0.99440	0.81280	0.98860	0.98570
31	${}^{E}\mathbb{H}^{DN}$	0.17890	0.00110	0.00150	0.99470	0.82020	0.98910	0.98700
32	${}^{E}\mathbb{H}^{DD}$	0.17850	0.00110	0.00150	0.99480	0.82270	0.98930	0.98770
33	${}^{U}\mathbb{H}^{AA}$	0.15820	0.00100	0.00140	0.99580	0.83250	0.99150	0.99060
34	${}^{U}\mathbb{H}^{AI}$	0.15840	0.00100	0.00140	0.99570	0.83000	0.99130	0.99030
35	${}^{U}\mathbb{H}^{AN}$	0.15680	0.00100	0.00130	0.99600	0.83740	0.99180	0.99160
36	${}^{U}\mathbb{H}^{AD}$	0.15640	0.00090	0.00130	0.99610	0.83990	0.99200	0.99320
37	${}^{U}\mathbb{H}^{IA}$	0.15840	0.00100	0.00140	0.99580	0.83990	0.99170	0.98910
38	${}^{U}\mathbb{H}^{II}$	0.15860	0.00100	0.00140	0.99570	0.83740	0.99150	0.98880
39	${}^{U}\mathbb{H}^{IN}$	0.15660	0.00090	0.00130	0.99600	0.84730	0.99200	0.99020
40	${}^{U}\mathbb{H}^{ID}$	0.15610	0.00090	0.00130	0.99620	0.84980	0.99220	0.99190
41	${}^{U}\mathbb{H}^{NA}$	0.15740	0.00100	0.00140	0.99600	0.85220	0.99180	0.98190
42	${}^{U}\mathbb{H}^{NI}$	0.15770	0.00100	0.00140	0.99590	0.84980	0.99160	0.98160
43	${}^{U}\mathbb{H}^{NN}$	0.15640	0.00090	0.00130	0.99620	0.85470	0.99210	0.98290
44	${}^{U}\mathbb{H}^{ND}$	0.15600	0.00090	0.00130	0.99630	0.85710	0.99230	0.98480
45	${}^{U}\mathbb{H}^{DA}$	0.15350	0.00100	0.00140	0.99610	0.84480	0.99200	0.98570
46	${}^{U}\mathbb{H}^{DI}$	0.15380	0.00100	0.00140	0.99600	0.84240	0.99180	0.98540
47	${}^{U}\mathbb{H}^{DN}$	0.15230	0.00090	0.00130	0.99630	0.84980	0.99230	0.98670
48	${}^{U}\mathbb{H}^{DD}$	0.15190	0.00090	0.00130	0.99640	0.85220	0.99250	0.98860
49	${}^{TG}\mathbb{H}^{AA}$	0.23090	0.00150	0.00210	0.99080	0.70200	0.98180	0.98940
50	${}^{TG}\mathbb{H}^{AI}$	0.23110	0.00150	0.00210	0.99070	0.69950	0.98160	0.98910
51	${}^{TG}\mathbb{H}^{AN}$	0.23040	0.00150	0.00200	0.99100	0.70440	0.98200	0.99010

Table 9. *Cont.*

S.No	Model	MAPE	MAE	RMSE	CORR	DA	NSE	KGE
52	${}^{TG}\mathbb{H}^{AD}$	0.23010	0.00140	0.00200	0.99110	0.70690	0.98220	0.99050
53	${}^{TG}\mathbb{H}^{IA}$	0.21630	0.00140	0.00190	0.99230	0.69460	0.98470	0.98820
54	${}^{TG}\mathbb{H}^{II}$	0.21650	0.00140	0.00190	0.99220	0.69210	0.98450	0.98790
55	${}^{TG}\mathbb{H}^{IN}$	0.21600	0.00140	0.00180	0.99250	0.69700	0.98490	0.98910
56	${}^{TG}\mathbb{H}^{ID}$	0.21570	0.00130	0.00180	0.99260	0.69950	0.98510	0.99000
57	${}^{TG}\mathbb{H}^{NA}$	0.29990	0.00190	0.00260	0.98500	0.73150	0.97010	0.97670
58	${}^{TG}\mathbb{H}^{NI}$	0.30020	0.00200	0.00260	0.98490	0.72910	0.96990	0.97640
59	${}^{TG}\mathbb{H}^{NN}$	0.29940	0.00190	0.00250	0.98520	0.73400	0.97030	0.97760
60	${}^{TG}\mathbb{H}^{ND}$	0.29900	0.00190	0.00250	0.98530	0.73650	0.97050	0.97850
61	${}^{TG}\mathbb{H}^{DA}$	0.30490	0.00200	0.00270	0.98480	0.72660	0.96930	0.96110
62	${}^{TG}\mathbb{H}^{DI}$	0.30520	0.00200	0.00270	0.98470	0.72410	0.96910	0.96080
63	${}^{TG}\mathbb{H}^{DN}$	0.30450	0.00190	0.00260	0.98500	0.72910	0.96950	0.96220
64	${}^{TG}\mathbb{H}^{DD}$	0.30410	0.00190	0.00260	0.98510	0.73150	0.96970	0.96330

Table 10. The out-of-sample one-step-ahead forecasting accuracy of all sixty-four hybrid models for the USD/CNY employing the proposed forecasting framework.

S.No	Model	MAPE	MAE	RMSE	CORR	DA	NSE	KGE
1	${}^{G}\mathbb{H}^{AA}$	0.08770	0.00630	0.01060	0.98990	0.62320	0.97990	0.98680
2	${}^{G}\mathbb{H}^{AI}$	0.04850	0.00350	0.00560	0.99730	0.75370	0.99440	0.98730
3	${}^{G}\mathbb{H}^{AN}$	0.07280	0.00520	0.00840	0.99380	0.68970	0.98760	0.98870
4	${}^{G}\mathbb{H}^{AD}$	0.07210	0.00520	0.00830	0.99380	0.69950	0.98770	0.98790
5	${}^{G}\mathbb{H}^{IA}$	0.06700	0.00480	0.00820	0.99410	0.67490	0.98820	0.98790
6	${}^{G}\mathbb{H}^{II}$	0.03820	0.00270	0.00430	0.99840	0.76350	0.99670	0.98850
7	${}^{G}\mathbb{H}^{IN}$	0.05310	0.00380	0.00610	0.99670	0.72170	0.99340	0.98920
8	${}^{G}\mathbb{H}^{ID}$	0.05270	0.00380	0.00610	0.99670	0.73890	0.99340	0.98830
9	${}^{G}\mathbb{H}^{NA}$	0.11350	0.00820	0.01340	0.98410	0.58620	0.96840	0.97470
10	${}^{G}\mathbb{H}^{NI}$	0.07310	0.00520	0.00810	0.99440	0.75120	0.98840	0.97310
11	${}^{G}\mathbb{H}^{NN}$	0.10730	0.00770	0.01210	0.98690	0.64290	0.97390	0.97650
12	${}^{G}\mathbb{H}^{ND}$	0.10710	0.00770	0.01210	0.98690	0.65020	0.97390	0.97570
13	${}^{G}\mathbb{H}^{DA}$	0.12330	0.00890	0.01380	0.98360	0.57640	0.96650	0.95200
14	${}^{G}\mathbb{H}^{DI}$	0.08810	0.00630	0.00900	0.99380	0.74140	0.98550	0.94810
15	${}^{G}\mathbb{H}^{DN}$	0.11700	0.00840	0.01260	0.98650	0.63790	0.97200	0.95290
16	${}^{G}\mathbb{H}^{DD}$	0.11690	0.00840	0.01260	0.98650	0.64780	0.97210	0.95210
17	${}^{E}\mathbb{H}^{AA}$	0.06270	0.00450	0.00700	0.99570	0.73890	0.99130	0.98500
18	${}^{E}\mathbb{H}^{AI}$	0.04040	0.00290	0.00460	0.99810	0.79310	0.99620	0.99170
19	${}^{E}\mathbb{H}^{AN}$	0.06350	0.00460	0.00700	0.99560	0.74880	0.99120	0.98720
20	${}^{E}\mathbb{H}^{AD}$	0.06260	0.00440	0.00690	0.99580	0.73890	0.99150	0.98620
21	${}^{E}\mathbb{H}^{IA}$	0.06280	0.00450	0.00700	0.99570	0.74630	0.99130	0.98560
22	${}^{E}\mathbb{H}^{II}$	0.04010	0.00290	0.00460	0.99810	0.79060	0.99620	0.99240
23	${}^{E}\mathbb{H}^{IN}$	0.06360	0.00460	0.00710	0.99560	0.74140	0.99120	0.98790
24	${}^{E}\mathbb{H}^{ID}$	0.06290	0.00450	0.00700	0.99570	0.74380	0.99140	0.98680
25	${}^{E}\mathbb{H}^{NA}$	0.07520	0.00540	0.00810	0.99430	0.71920	0.98820	0.97540
26	${}^{E}\mathbb{H}^{NI}$	0.05030	0.00360	0.00550	0.99750	0.76850	0.99470	0.98140
27	${}^{E}\mathbb{H}^{NN}$	0.07500	0.00540	0.00810	0.99430	0.71430	0.98840	0.97760
28	${}^{E}\mathbb{H}^{ND}$	0.07360	0.00530	0.00800	0.99440	0.71670	0.98860	0.97650
29	${}^{E}\mathbb{H}^{DA}$	0.07800	0.00560	0.00840	0.99390	0.71430	0.98740	0.97260
30	${}^{E}\mathbb{H}^{DI}$	0.05240	0.00380	0.00570	0.99730	0.76350	0.99420	0.97850
31	${}^{E}\mathbb{H}^{DN}$	0.07780	0.00560	0.00840	0.99400	0.71920	0.98760	0.97480
32	${}^{E}\mathbb{H}^{DD}$	0.07650	0.00550	0.00830	0.99410	0.71670	0.98780	0.97370
33	${}^{U}\mathbb{H}^{AA}$	0.05310	0.00380	0.00610	0.99670	0.76600	0.99340	0.99040
34	${}^{U}\mathbb{H}^{AI}$	0.04240	0.00300	0.00510	0.99770	0.77340	0.99540	0.99680
35	${}^{U}\mathbb{H}^{AN}$	0.05380	0.00390	0.00620	0.99660	0.77340	0.99320	0.99170
36	${}^{U}\mathbb{H}^{AD}$	0.05580	0.00400	0.00640	0.99640	0.76110	0.99280	0.99260
37	${}^{U}\mathbb{H}^{IA}$	0.05330	0.00380	0.00590	0.99690	0.76110	0.99380	0.99100
38	${}^{U}\mathbb{H}^{II}$	0.04300	0.00310	0.00490	0.99790	0.77090	0.99570	0.99730

Table 10. *Cont.*

S.No	Model	MAPE	MAE	RMSE	CORR	DA	NSE	KGE
39	${}^{U}\mathbb{H}^{IN}$	0.05400	0.00390	0.00600	0.99680	0.75620	0.99360	0.99230
40	${}^{U}\mathbb{H}^{ID}$	0.05620	0.00400	0.00610	0.99670	0.76110	0.99330	0.99320
41	${}^{U}\mathbb{H}^{NA}$	0.06420	0.00460	0.00690	0.99610	0.76600	0.99170	0.97200
42	${}^{U}\mathbb{H}^{NI}$	0.05040	0.00360	0.00550	0.99760	0.77830	0.99470	0.97840
43	${}^{U}\mathbb{H}^{NN}$	0.06480	0.00470	0.00690	0.99600	0.76850	0.99150	0.97340
44	${}^{U}\mathbb{H}^{ND}$	0.06640	0.00480	0.00700	0.99590	0.75860	0.99130	0.97440
45	${}^{U}\mathbb{H}^{DA}$	0.06390	0.00460	0.00680	0.99630	0.77090	0.99180	0.96970
46	${}^{U}\mathbb{H}^{DI}$	0.05030	0.00360	0.00550	0.99760	0.77590	0.99470	0.97630
47	${}^{U}\mathbb{H}^{DN}$	0.06460	0.00460	0.00690	0.99610	0.77340	0.99170	0.97120
48	${}^{U}\mathbb{H}^{DD}$	0.06600	0.00470	0.00700	0.99600	0.75620	0.99140	0.97220
49	${}^{TG}\mathbb{H}^{AA}$	0.08700	0.00620	0.01050	0.99020	0.62320	0.98050	0.98710
50	${}^{TG}\mathbb{H}^{AI}$	0.04720	0.00340	0.00550	0.99740	0.76110	0.99470	0.98810
51	${}^{TG}\mathbb{H}^{AN}$	0.07260	0.00520	0.00830	0.99390	0.68970	0.98790	0.98900
52	${}^{TG}\mathbb{H}^{AD}$	0.07180	0.00520	0.00830	0.99390	0.69460	0.98790	0.98820
53	${}^{TG}\mathbb{H}^{IA}$	0.06610	0.00470	0.00800	0.99430	0.67730	0.98850	0.98770
54	${}^{TG}\mathbb{H}^{II}$	0.03870	0.00280	0.00450	0.99830	0.76350	0.99650	0.98890
55	${}^{TG}\mathbb{H}^{IN}$	0.05370	0.00390	0.00620	0.99660	0.72410	0.99330	0.98920
56	${}^{TG}\mathbb{H}^{ID}$	0.05310	0.00380	0.00620	0.99660	0.73400	0.99320	0.98830
57	${}^{TG}\mathbb{H}^{NA}$	0.11330	0.00810	0.01330	0.98420	0.58130	0.96860	0.97480
58	${}^{TG}\mathbb{H}^{NI}$	0.07230	0.00520	0.00800	0.99450	0.75370	0.98860	0.97360
59	${}^{TG}\mathbb{H}^{NN}$	0.10720	0.00770	0.01210	0.98700	0.64780	0.97400	0.97670
60	${}^{TG}\mathbb{H}^{ND}$	0.10700	0.00770	0.01210	0.98700	0.65270	0.97400	0.97590
61	${}^{TG}\mathbb{H}^{DA}$	0.12400	0.00890	0.01370	0.98360	0.58370	0.96670	0.95220
62	${}^{TG}\mathbb{H}^{DI}$	0.08610	0.00620	0.00880	0.99420	0.75620	0.98630	0.94850
63	${}^{TG}\mathbb{H}^{DN}$	0.11780	0.00850	0.01260	0.98640	0.64780	0.97200	0.95330
64	${}^{TG}\mathbb{H}^{DD}$	0.11760	0.00840	0.01260	0.98640	0.65270	0.97200	0.95240

Similarly, the three best forecasting models for the USD/CNY exchange rate (Table 10) are ${}^{G}\mathbb{H}^{II}$, ${}^{TG}\mathbb{H}^{II}$, and ${}^{E}\mathbb{H}^{II}$. Of these, the Gaussian kernel-based model ${}^{G}\mathbb{H}^{II}$ performs the best overall in forecasting with MAPE = 0.0382, MAE = 0.0027, RMSE = 0.0043, CORR = 0.9984, NSE = 0.9967, KGE = 0.9885, and DA = 0.7635. The truncated Gaussian model ${}^{TG}\mathbb{H}^{II}$ with MAPE = 0.0387, RMSE = 0.0045, CORR = 0.9983, and NSE = 0.9965 has the second-best forecasting accuracy. The Epanechnikov kernel specification ${}^{E}\mathbb{H}^{II}$ is a competitive specification with MAPE = 0.0401, RMSE = 0.0046, CORR = 0.9981, and NSE = 0.9962. Similarly, these results indicate the utility of ARIMA-based forecasting structures in capturing persistent temporal dynamics and the relatively smoother behavior of the USD/CNY exchange rate series. Hence, across all five exchange-rate markets, the proposed kernel regression-based hybrid models consistently ranked among the best-performing forecasting approaches. The Epanechnikov kernel, combined with ARIMA-NNAR or NNAR-NNAR forecasting structures, frequently produced the lowest forecast errors. The only exception was the USD/CNY market, where Gaussian-kernel decomposition with ARIMA models achieved the best performance.

In addition to the above, the comparative results in Table 11 reveal that the direct hybrid forecasting framework generally yields poorer predictive performance than the proposed kernel regression-based decomposition framework. The direct hybrid models differ from the decomposition-driven approach in that forecasting techniques are applied directly to the raw exchange-rate series without separating long-run trend structures from high-frequency stochastic fluctuations. As a result, across all five markets, decomposition-based hybrid models consistently outperformed direct hybrid forecasting. The improvement was particularly pronounced for USD/CNY, where the proposed Gaussian-kernel model reduced MAPE, MAE, and RMSE by approximately 74%, 74%, and 76%, respectively. Similar improvements were observed for GBP/USD, EUR/USD, AUD/USD, and USD/JPY,

demonstrating that decomposition prior to forecasting substantially enhances predictive accuracy. It should be emphasized that the benchmark hybrid models are applied directly to the original exchange-rate series, whereas the proposed methodology integrates kernel regression decomposition as an inherent component of the forecasting framework. Therefore, the reported comparisons evaluate the effectiveness of the complete decomposition-based hybrid forecasting framework rather than the forecasting models alone. The observed improvements consequently quantify the additional predictive benefit obtained by introducing adaptive kernel regression decomposition prior to component-wise forecasting.

Finally, we compare with the single forecasting models reported in Table 12, namely, AR, ARIMA, NPAR, and NNAR, and find that the proposed kernel regression decomposition-based hybrid forecasting framework is superior across all foreign exchange markets. In conclusion, the empirical results strongly indicate that the new kernel regression decomposition-based hybrid forecasting framework outperforms both direct hybridization approaches and single forecasting models in all foreign exchange markets. The significant reductions in forecasting errors and improvements in forecasting efficiency confirm the robustness, flexibility and generalizability of the proposed methodology for modeling complex nonlinear and nonstationary financial time series.

Table 11. Out-of-sample one-step-ahead forecasting performance of direct hybrid models (without decomposition) across different foreign exchange markets.

S.No	Model	MAPE	MAE	RMSE	CORR	DA	NSE	KGE
				EUR/USD				
1	AR+AR	0.3554	0.0038	0.0052	0.9931	0.9428	0.9914	0.9929
2	ARIMA+AR	0.3555	0.0038	0.0052	0.9930	0.9419	0.9912	0.9927
3	NPAR+AR	0.3556	0.0038	0.0053	0.9929	0.9412	0.9910	0.9925
4	NNAR+AR	0.3552	0.0038	0.0052	0.9930	0.9421	0.9911	0.9928
5	AR+ARIMA	0.3555	0.0038	0.0052	0.9930	0.9419	0.9912	0.9927
6	ARIMA+ARIMA	0.3557	0.0039	0.0053	0.9928	0.9404	0.9908	0.9923
7	NPAR+ARIMA	0.3558	0.0039	0.0053	0.9928	0.9400	0.9907	0.9922
8	NNAR+ARIMA	0.3554	0.0038	0.0052	0.9929	0.9415	0.9910	0.9926
9	AR+NPAR	0.3556	0.0038	0.0053	0.9929	0.9412	0.9910	0.9925
10	ARIMA+NPAR	0.3558	0.0039	0.0053	0.9928	0.9400	0.9907	0.9922
11	NPAR+NPAR	0.3561	0.0039	0.0053	0.9927	0.9387	0.9904	0.9919
12	NNAR+NPAR	0.3559	0.0039	0.0053	0.9927	0.9391	0.9905	0.9920
13	AR+NNAR	0.3552	0.0038	0.0052	0.9930	0.9421	0.9911	0.9928
14	ARIMA+NNAR	0.3554	0.0038	0.0052	0.9929	0.9415	0.9910	0.9926
15	NPAR+NNAR	0.3559	0.0039	0.0053	0.9927	0.9391	0.9905	0.9920
16	NNAR+NNAR	0.3557	0.0039	0.0053	0.9927	0.9395	0.9906	0.9921
				USD/JPY				
17	AR+AR	0.5148	0.7724	1.0172	0.9768	0.8614	0.9736	0.9758
18	ARIMA+AR	0.5151	0.7728	1.0178	0.9766	0.8597	0.9732	0.9754
19	NPAR+AR	0.5158	0.7736	1.0186	0.9765	0.8582	0.9729	0.9751
20	NNAR+AR	0.5224	0.7835	1.0217	0.9760	0.8514	0.9712	0.9735
21	AR+ARIMA	0.5151	0.7728	1.0178	0.9766	0.8597	0.9732	0.9754
22	ARIMA+ARIMA	0.5155	0.7733	1.0181	0.9765	0.8589	0.9730	0.9752
23	NPAR+ARIMA	0.5160	0.7739	1.0184	0.9765	0.8578	0.9728	0.9750
24	NNAR+ARIMA	0.5211	0.7818	1.0209	0.9761	0.8526	0.9715	0.9738
25	AR+NPAR	0.5158	0.7736	1.0186	0.9765	0.8582	0.9729	0.9751
26	ARIMA+NPAR	0.5160	0.7739	1.0184	0.9765	0.8578	0.9728	0.9750
27	NPAR+NPAR	0.5172	0.7755	1.0198	0.9762	0.8551	0.9721	0.9744
28	NNAR+NPAR	0.5238	0.7856	1.0236	0.9758	0.8490	0.9706	0.9729
29	AR+NNAR	0.5224	0.7835	1.0217	0.9760	0.8514	0.9712	0.9735
30	ARIMA+NNAR	0.5211	0.7818	1.0209	0.9761	0.8526	0.9715	0.9738
31	NPAR+NNAR	0.5238	0.7856	1.0236	0.9758	0.8490	0.9706	0.9729
32	NNAR+NNAR	0.5362	0.8048	1.0391	0.9749	0.8422	0.9688	0.9712

Table 11. *Cont.*

S.No	Model	MAPE	MAE	RMSE	CORR	DA	NSE	KGE
				AUD/USD				
33	AR+AR	0.4662	0.0029	0.0040	0.9638	0.8245	0.9608	0.9624
34	ARIMA+AR	0.4665	0.0029	0.0041	0.9636	0.8228	0.9604	0.9620
35	NPAR+AR	0.4660	0.0029	0.0040	0.9640	0.8258	0.9611	0.9627
36	NNAR+AR	0.4664	0.0029	0.0041	0.9637	0.8234	0.9605	0.9621
37	AR+ARIMA	0.4665	0.0029	0.0041	0.9636	0.8228	0.9604	0.9620
38	ARIMA+ARIMA	0.4676	0.0030	0.0041	0.9632	0.8195	0.9596	0.9613
39	NPAR+ARIMA	0.4668	0.0029	0.0041	0.9635	0.8219	0.9602	0.9618
40	NNAR+ARIMA	0.4670	0.0030	0.0041	0.9633	0.8206	0.9599	0.9615
41	AR+NPAR	0.4660	0.0029	0.0040	0.9640	0.8258	0.9611	0.9627
42	ARIMA+NPAR	0.4668	0.0029	0.0041	0.9635	0.8219	0.9602	0.9618
43	NPAR+NPAR	0.4672	0.0030	0.0041	0.9634	0.8201	0.9598	0.9614
44	NNAR+NPAR	0.4671	0.0030	0.0041	0.9633	0.8204	0.9599	0.9615
45	AR+NNAR	0.4664	0.0029	0.0041	0.9637	0.8234	0.9605	0.9621
46	ARIMA+NNAR	0.4670	0.0030	0.0041	0.9633	0.8206	0.9599	0.9615
47	NPAR+NNAR	0.4671	0.0030	0.0041	0.9633	0.8204	0.9599	0.9615
48	NNAR+NNAR	0.4674	0.0030	0.0041	0.9631	0.8188	0.9594	0.9611
				USD/CNY				
49	AR+AR	0.1458	0.0104	0.0181	0.9705	0.8426	0.9678	0.9694
50	ARIMA+AR	0.1460	0.0104	0.0181	0.9704	0.8418	0.9676	0.9692
51	NPAR+AR	0.1512	0.0108	0.0182	0.9701	0.8374	0.9665	0.9681
52	NNAR+AR	0.1504	0.0107	0.0182	0.9701	0.8382	0.9667	0.9683
53	AR+ARIMA	0.1460	0.0104	0.0181	0.9704	0.8418	0.9676	0.9692
54	ARIMA+ARIMA	0.1462	0.0105	0.0182	0.9703	0.8409	0.9674	0.9690
55	NPAR+ARIMA	0.1509	0.0108	0.0181	0.9702	0.8388	0.9669	0.9685
56	NNAR+ARIMA	0.1498	0.0107	0.0182	0.9702	0.8395	0.9671	0.9687
57	AR+NPAR	0.1512	0.0108	0.0182	0.9701	0.8374	0.9665	0.9681
58	ARIMA+NPAR	0.1509	0.0108	0.0181	0.9702	0.8388	0.9669	0.9685
59	NPAR+NPAR	0.1586	0.0114	0.0184	0.9695	0.8312	0.9650	0.9667
60	NNAR+NPAR	0.1572	0.0113	0.0184	0.9696	0.8320	0.9653	0.9670
61	AR+NNAR	0.1504	0.0107	0.0182	0.9701	0.8382	0.9667	0.9683
62	ARIMA+NNAR	0.1498	0.0107	0.0182	0.9702	0.8395	0.9671	0.9687
63	NPAR+NNAR	0.1572	0.0113	0.0184	0.9696	0.8320	0.9653	0.9670
64	NNAR+NNAR	0.1564	0.0112	0.0184	0.9696	0.8328	0.9655	0.9672
				GBP/USD				
65	AR+AR	0.3668	0.0047	0.0061	0.9862	0.9184	0.9846	0.9868
66	ARIMA+AR	0.3670	0.0047	0.0062	0.9860	0.9161	0.9842	0.9863
67	NPAR+AR	0.3675	0.0048	0.0062	0.9859	0.9148	0.9839	0.9860
68	NNAR+AR	0.3672	0.0048	0.0062	0.9859	0.9152	0.9840	0.9861
69	AR+ARIMA	0.3670	0.0047	0.0062	0.9860	0.9161	0.9842	0.9863
70	ARIMA+ARIMA	0.3673	0.0048	0.0062	0.9858	0.9143	0.9838	0.9859
71	NPAR+ARIMA	0.3676	0.0048	0.0062	0.9858	0.9139	0.9837	0.9858
72	NNAR+ARIMA	0.3674	0.0048	0.0062	0.9858	0.9141	0.9838	0.9859
73	AR+NPAR	0.3675	0.0048	0.0062	0.9859	0.9148	0.9839	0.9860
74	ARIMA+NPAR	0.3676	0.0048	0.0062	0.9858	0.9139	0.9837	0.9858
75	NPAR+NPAR	0.3682	0.0048	0.0063	0.9856	0.9117	0.9832	0.9853
76	NNAR+NPAR	0.3679	0.0048	0.0062	0.9857	0.9128	0.9835	0.9856
77	AR+NNAR	0.3672	0.0048	0.0062	0.9859	0.9152	0.9840	0.9861
78	ARIMA+NNAR	0.3674	0.0048	0.0062	0.9858	0.9141	0.9838	0.9859
79	NPAR+NNAR	0.3679	0.0048	0.0062	0.9857	0.9128	0.9835	0.9856
80	NNAR+NNAR	0.3677	0.0048	0.0062	0.9857	0.9131	0.9836	0.9857

Table 12. Performance comparison of single forecasting models across different foreign exchange markets.

S.No	Model	MAPE	MAE	RMSE	CORR	DA	NSE	KGE
				EUR/USD				
1	AR	0.3568	0.0038	0.0052	0.9942	0.9432	0.9916	0.9931
2	ARIMA	0.3569	0.0038	0.0052	0.9941	0.9428	0.9915	0.9929
3	NPAR	0.3571	0.0039	0.0053	0.9939	0.9419	0.9912	0.9926
4	NNAR	0.3575	0.0039	0.0054	0.9936	0.9408	0.9908	0.9921
				USD/JPY				
5	AR	0.5173	0.7759	1.0208	0.9799	0.8625	0.9739	0.9763
6	ARIMA	0.5174	0.7762	1.0211	0.9797	0.8619	0.9737	0.9760
7	NPAR	0.5187	0.7781	1.0228	0.9791	0.8598	0.9730	0.9751
8	NNAR	0.5583	0.8388	1.0714	0.9752	0.8486	0.9691	0.9702
				AUD/USD				
9	AR	0.4676	0.0029	0.0040	0.9642	0.8261	0.9614	0.9632
10	ARIMA	0.4701	0.0030	0.0041	0.9631	0.8224	0.9601	0.9617
11	NPAR	0.4684	0.0029	0.0041	0.9638	0.8248	0.9609	0.9626
12	NNAR	0.4685	0.0030	0.0041	0.9636	0.8242	0.9607	0.9623
				USD/CNY				
13	AR	0.1471	0.0105	0.0181	0.9708	0.8435	0.9682	0.9698
14	ARIMA	0.1474	0.0106	0.0182	0.9706	0.8427	0.9679	0.9695
15	NPAR	0.1655	0.0119	0.0188	0.9689	0.8341	0.9651	0.9669
16	NNAR	0.1627	0.0117	0.0186	0.9695	0.8360	0.9658	0.9676
				GBP/USD				
17	AR	0.3683	0.0047	0.0061	0.9864	0.9195	0.9849	0.9872
18	ARIMA	0.3684	0.0047	0.0061	0.9863	0.9190	0.9847	0.9870
19	NPAR	0.3705	0.0048	0.0063	0.9856	0.9138	0.9835	0.9857
20	NNAR	0.3686	0.0047	0.0062	0.9861	0.9182	0.9844	0.9866

In addition to the conventional forecasting accuracy measures (MAPE, MAE, RMSE, CORR, NSE, KGE, and directional accuracy), the DM test was employed to determine whether the forecasting improvements achieved by the proposed kernel regression-based hybrid models are statistically significant relative to the best-performing direct hybrid and standalone benchmark models. The DM test was computed using the complete set of out-of-sample forecasts generated during the expanding-window evaluation period, and the resulting pairwise p-values are reported in Table 13. The reported values correspond to one-sided DM tests, where a p-value below 0.05 indicates that the forecasting model in the corresponding row significantly outperforms the model in the corresponding column. Overall, the DM test confirms that the forecasting improvements achieved by the proposed kernel regression-based hybrid models are statistically significant rather than resulting from random variation. The best-performing decomposition-based hybrid setups have quite high p-values, indicating statistically similar predictive performance. The best kernel regression-based hybrid models significantly outperform the equivalent direct hybrid and standalone benchmark models for the GBP/USD and EUR/USD exchange rates. The same pattern can be seen for the USD/JPY, AUD/USD and USD/CNY markets as well, where the leading kernel regression-based hybrid models outperform the conventional benchmark models consistently and significantly, while the differences among the best-performing decomposition-based hybrid configurations are still statistically insignificant. Overall, the DM test demonstrates the effectiveness of the proposed kernel regression based decomposition framework with robust statistical evidence in all the five foreign exchange markets. Several kernel regression-based hybrid configurations yield statistically indistinguishable forecasting performance but consistently and significantly outperform

the corresponding direct hybrid and standalone forecasting models. These results further support the forecasting accuracy results and confirm that the improvements seen are real increases in predictive performance and not due to random sampling variation.

Table 13. The DM test results (*p*-values) comparing the proposed kernel regression-based hybrid models with the best direct hybrid and standalone benchmark models across the five foreign exchange markets.

GBP/USD					
Models	$^{E}\mathbb{H}^{ID}$	$^{U}\mathbb{H}^{ID}$	$^{TG}\mathbb{H}^{ID}$	AR+ARIMA	AR
$^{E}\mathbb{H}^{ID}$	–	0.120	0.005	0.001	0.001
$^{U}\mathbb{H}^{ID}$	0.880	–	0.020	0.001	0.001
$^{TG}\mathbb{H}^{ID}$	0.995	0.980	–	0.030	0.040
AR+ARIMA	0.999	0.999	0.970	–	0.850
AR	0.999	0.999	0.960	0.150	–
EUR/USD					
Models	$^{E}\mathbb{H}^{ID}$	$^{U}\mathbb{H}^{ID}$	$^{TG}\mathbb{H}^{ID}$	NNAR+AR	AR
$^{E}\mathbb{H}^{ID}$	–	0.090	0.040	0.001	0.001
$^{U}\mathbb{H}^{ID}$	0.910	–	0.280	0.002	0.002
$^{TG}\mathbb{H}^{ID}$	0.960	0.720	–	0.003	0.004
NNAR+AR	0.999	0.998	0.997	–	0.840
AR	0.999	0.998	0.996	0.160	–
USD/JPY					
Models	$^{E}\mathbb{H}^{ID}$	$^{E}\mathbb{H}^{IN}$	$^{E}\mathbb{H}^{II}$	AR+AR	AR
$^{E}\mathbb{H}^{ID}$	–	0.420	0.310	0.001	0.001
$^{E}\mathbb{H}^{IN}$	0.580	–	0.460	0.001	0.001
$^{E}\mathbb{H}^{II}$	0.690	0.540	–	0.002	0.002
AR+AR	0.999	0.999	0.998	–	0.850
AR	0.999	0.999	0.998	0.150	–
AUD/USD					
Models	$^{E}\mathbb{H}^{ID}$	$^{U}\mathbb{H}^{ID}$	$^{TG}\mathbb{H}^{ID}$	AR+NPAR	AR
$^{E}\mathbb{H}^{ID}$	–	0.100	0.005	0.001	0.001
$^{U}\mathbb{H}^{ID}$	0.900	–	0.050	0.002	0.002
$^{TG}\mathbb{H}^{ID}$	0.995	0.950	–	0.020	0.030
AR+NPAR	0.999	0.998	0.980	–	0.850
AR	0.999	0.998	0.970	0.150	–
USD/CNY					
Models	$^{G}\mathbb{H}^{II}$	$^{E}\mathbb{H}^{II}$	$^{U}\mathbb{H}^{AI}$	AR+AR	AR
$^{G}\mathbb{H}^{II}$	–	0.420	0.080	0.001	0.001
$^{E}\mathbb{H}^{II}$	0.580	–	0.210	0.001	0.001
$^{U}\mathbb{H}^{AI}$	0.920	0.790	–	0.002	0.002
AR+AR	0.999	0.999	0.998	–	0.860
AR	0.999	0.999	0.998	0.140	–

To evaluate the robustness of the proposed kernel regression decomposition framework with respect to bandwidth selection, a bandwidth sensitivity analysis was conducted by varying the bandwidth around the least-squares cross-validation (LSCV) optimum. Specifically, the complete forecasting framework was re-estimated using bandwidths equal to $0.8h^*$, h^*, and $1.2h^*$, where h^* denotes the bandwidth selected automatically by the LSCV criterion. Since the LSCV-selected bandwidth produced the lowest forecasting error for

every exchange-rate series, Table 14 reports the percentage increase in MAPE obtained under the two alternative bandwidth specifications relative to the optimal bandwidth.

Overall, the proposed forecasting framework exhibits only limited sensitivity to moderate bandwidth perturbations. Across all five foreign exchange markets, changing the bandwidth by ±20% around the LSCV optimum results in only small increases in forecasting error, ranging from 1.7% to 3.6%. These results indicate that the predictive performance of the proposed kernel regression decomposition framework remains stable even when the bandwidth deviates moderately from its optimal value, demonstrating that the forecasting accuracy does not depend critically on precise bandwidth tuning.

The degree of sensitivity also reflects the statistical properties of the individual exchange rate markets. The USD/JPY market shows the largest increase in MAPE (3.1–3.6%), which is in line with its relatively larger forecasting errors and stronger short-run volatility found throughout the empirical analysis. By contrast, an exchange rate USD/CNY is the least sensitive (1.7–2.0%), which can be attributed to its relatively smoother market dynamics and lower forecasting errors. The other exchange-rate markets (GBP/USD, EUR/USD and AUD/USD) are of moderate sensitivity, with increases in forecasting errors remaining below 3%, in line with their moderate levels of market volatility. These results indicate that the choice of the optimal bandwidths naturally varies across the exchange-rate series, due to differences in the local smoothness, volatility, and dependence over time of the series themselves, and not due to instability in the proposed methodology. Since bandwidth selection is performed automatically using the LSCV criterion, the kernel regression decomposition adapts to the statistical characteristics of each exchange-rate market without requiring manual parameter tuning. Consequently, the proposed decomposition framework exhibits both strong adaptability and robustness across heterogeneous foreign exchange markets, thereby supporting its applicability for practical forecasting under different market conditions.

Table 14. Percentage increase in MAPE relative to the optimal bandwidth (h^*) selected by the least-squares cross-validation (LSCV) criterion under moderate bandwidth perturbations.

Exchange-Rate Market	0.8 h^*	1.2 h^*
GBP/USD	+1.9%	+2.4%
EUR/USD	+2.3%	+2.8%
USD/JPY	+3.1%	+3.6%
AUD/USD	+2.2%	+2.5%
USD/CNY	+1.7%	+2.0%

4. Discussion, Limitations, and Future Research

This section compares the forecasting performance of the proposed kernel regression-based hybrid framework with representative state-of-the-art forecasting models reported in the literature for the five major foreign exchange markets. The comparison is based on MAPE, MAE, and RMSE, where smaller values indicate superior predictive performance. As reported in Table 15, the proposed decomposition-based framework consistently achieves the lowest forecasting errors across all exchange-rate markets. For the GBP/USD exchange rate, the proposed ${}^{E}\mathbb{H}^{ID}$ model produces the smallest forecasting errors (MAPE = 0.08490, MAE = 0.00090, and RMSE = 0.00120), reducing MAPE by approximately 16% relative to the strongest competing model SRFxy [60] and by more than 50% compared with HPF23 [30]. A similar pattern is observed for the remaining exchange-rate markets. For EUR/USD, USD/JPY, AUD/USD, and USD/CNY, the proposed framework consistently outperforms all competing forecasting approaches, including HPF23 [30], C23 [61], SRFxy [60], and LRNPAR [7]. The largest forecasting improvements are obtained for the highly volatile USD/JPY market, whereas the gains for USD/CNY are relatively

smaller because of its more regulated exchange-rate regime and smoother market dynamics. Nevertheless, the proposed framework delivers the best forecasting performance for all five markets. Thus, these results indicate that the proposed kernel regression decomposition can successfully disentangle the long-run exchange-rate movements from the short-run nonlinear fluctuations so that the subsequent hybrid forecasting models can better capture the heterogeneous dynamics of each component. Unlike conventional decomposition methods that require pre-specifying basis functions, frequency bands, or iteratively extracting modes, kernel regression directly estimates the underlying trend by adaptive local smoothing.

Table 15. The mean accuracy errors of the proposed method are compared with those reported in the existing literature across all FX markets considered.

Market	Model	MAPE	MAE	RMSE
GBP/USD	$^{\mathbf{E}}\mathbb{H}^{\mathbf{ID}}$ (Proposed)	0.08490	0.00090	0.00120
	HPF23 [30]	0.19240	0.00311	0.00325
	C23 [61]	0.11320	0.00253	0.00294
	SRFxy [60]	0.10121	0.00165	0.00210
	LRNPAR [7]	0.11613	0.00198	0.00252
EUR/USD	$^{\mathbf{E}}\mathbb{H}^{\mathbf{ID}}$ (Proposed)	0.12920	0.00137	0.00187
	HPF23 [30]	0.29290	0.00474	0.00507
	C23 [61]	0.17230	0.00385	0.00459
	SRFxy [60]	0.15400	0.00251	0.00328
	LRNPAR [7]	0.17680	0.00301	0.00393
USD/JPY	$^{\mathbf{D}}\mathbb{H}^{\mathbf{II}}$ (Proposed)	0.03820	0.00270	0.00430
	HPF23 [30]	0.39600	0.90680	0.91570
	C23 [61]	0.23280	0.73590	0.82870
	SRFxy [60]	0.20810	0.47970	0.59230
	LRNPAR [7]	0.23890	0.57560	0.71030
AUD/USD	$^{\mathbf{E}}\mathbb{H}^{\mathbf{ID}}$ (Proposed)	0.09780	0.00100	0.00130
	HPF23 [30]	0.22180	0.00360	0.00352
	C23 [61]	0.13040	0.00292	0.00318
	SRFxy [60]	0.11660	0.00190	0.00227
	LRNPAR [7]	0.13380	0.00228	0.00272
USD/CNY	$^{\mathbf{E}}\mathbb{H}^{\mathbf{ID}}$ (Proposed)	0.06290	0.00450	0.00700
	HPF23 [30]	0.14270	0.01620	0.01890
	C23 [61]	0.08390	0.01310	0.01710
	SRFxy [60]	0.07500	0.00855	0.01220
	LRNPAR [7]	0.08610	0.01026	0.01460

In addition to the forecasting accuracy measures, the DM test was used to check the statistical significance of the observed forecasting improvements. The pairwise DM test results comparing the proposed framework with representative benchmark forecasting models across all exchange-rate markets are reported in Table 16. The consistently small p-values from comparisons with the proposed model provide strong statistical evidence that the observed forecasting improvements are not due to random variation. Conversely, the p-values obtained from pairwise comparisons between benchmark forecasting models are typically much larger, suggesting that their predictive performance is statistically indistinguishable. The results improve forecasting accuracy metrics and provide statistical and practical support for the superiority of the proposed framework across a variety of foreign exchange markets.

Table 16. The DM test results compare the proposed model against the best forecasting models in the literature across all exchange rate markets.

GBP/USD					
Models	$^{E}\mathbb{H}^{ID}$	HPF23	C23	SRFxy	LRNPAR
$^{E}\mathbb{H}^{ID}$	–	0.001	0.001	0.003	0.002
HPF23	0.999	–	0.210	0.090	0.180
C23	0.999	0.790	–	0.240	0.410
SRFxy	0.997	0.910	0.760	–	0.320
LRNPAR	0.998	0.820	0.590	0.680	–
EUR/USD					
Models	$^{E}\mathbb{H}^{ID}$	HPF23	C23	SRFxy	LRNPAR
$^{E}\mathbb{H}^{ID}$	–	0.001	0.001	0.002	0.001
HPF23	0.999	–	0.180	0.100	0.260
C23	0.999	0.820	–	0.280	0.450
SRFxy	0.998	0.900	0.720	–	0.360
LRNPAR	0.999	0.740	0.550	0.640	–
USD/JPY					
Models	$^{E}\mathbb{H}^{ID}$	HPF23	C23	SRFxy	LRNPAR
$^{G}\mathbb{H}^{II}$	–	0.001	0.001	0.004	0.002
HPF23	0.999	–	0.150	0.070	0.210
C23	0.999	0.850	–	0.250	0.390
SRFxy	0.996	0.930	0.750	–	0.340
LRNPAR	0.998	0.790	0.610	0.660	–
AUD/USD					
Models	$^{E}\mathbb{H}^{ID}$	HPF23	C23	SRFxy	LRNPAR
$^{E}\mathbb{H}^{ID}$	–	0.001	0.001	0.002	0.001
HPF23	0.999	–	0.230	0.110	0.240
C23	0.999	0.770	–	0.260	0.420
SRFxy	0.998	0.890	0.740	–	0.310
LRNPAR	0.999	0.760	0.580	0.690	–
USD/CNY					
Models	$^{E}\mathbb{H}^{ID}$	HPF23	C23	SRFxy	LRNPAR
$^{E}\mathbb{H}^{ID}$	–	0.001	0.001	0.003	0.002
HPF23	0.999	–	0.190	0.090	0.270
C23	0.999	0.810	–	0.220	0.390
SRFxy	0.997	0.910	0.780	–	0.330
LRNPAR	0.998	0.730	0.610	0.670	–

The main reason for the better performance of the proposed method in terms of financial time series is the characteristics of the kernel regression decomposition. Kernel regression estimates the underlying trend in a nonparametric way, thus avoiding restrictive functional assumptions and adapting in a natural way to the local behavior of the exchange-rate series. Thus, the decomposition isolates persistent long-run market evolution from localized nonlinear fluctuations without predefined basis functions, frequency-band selection, or iterative decomposition procedures. Moreover, the estimated trend and residual components have sufficiently different statistical properties such that the persistent long-run dynamics can be captured by linear time-series models, while the nonlinear learning algorithms can capture the asymmetric and volatility-clustered behavior embedded in the residual component. The proposed framework is characterized by these methodological

features and differs from decomposition techniques (EMD, VMD, STL, and wavelet transforms) so that it provides a flexible foundation for hybrid forecasting of nonlinear and nonstationary financial time series.

The empirical results further support the proposed interpretation of symmetry–asymmetry. The adaptive kernel regression yields a smooth and relatively symmetric long-run trend consistent with the market equilibrium, while the residual component captures asymmetric short-run market behavior such as volatility clustering, abrupt price changes, and nonlinear adjustments. The proposed hybrid forecasting framework separately models these heterogeneous temporal structures, enabling specialized forecasting models to better utilize the distinct statistical properties of each component. Thus, the generalized forecasting enhancements observed across all five currency markets suggest that an explicit decomposition of long-run symmetric dynamics and short-run asymmetric fluctuations provides a more informative description of exchange rate behavior than forecasting the raw series.

The proposed framework outperforms existing forecasting methods across all exchange-rate markets considered in this study. Nevertheless, some limitations should be acknowledged. The empirical analysis is restricted to five major foreign exchange markets and one-step-ahead forecasting. Thus, the reported results should not be interpreted to be valid for all financial markets and forecasting horizons. Also, while the proposed kernel regression decomposition shows relatively low parameter sensitivity, the forecasting performance may still vary in substantially different market conditions or structural regimes. Such limitations motivate future research to extend the proposed framework to direct and recursive multi-step forecasting horizons, enabling medium- and long-term exchange-rate prediction for broader financial planning, investment, and risk management applications. Moreover, the robustness of the proposed methodology will be examined using major historical financial crises, such as the 2008 Global Financial Crisis and the 1997 Asian Financial Crisis, to further assess its stability under extreme market conditions and structural breaks. Another promising direction of research is the combination of kernel regression decomposition with recent regime-switching and bilinear models for volatility, such as bispectral bilinear Markov chain models and Markov-switching medium-threshold BLGARCH models [62,63]. Frameworks can further improve the ability to capture abrupt regime switches, nonlinear market dynamics, and periods of heightened volatility, thereby improving exchange-rate forecasting in complex financial environments.

5. Concluding Remarks

In this paper, we proposed a hybrid forecasting framework based on kernel regression decomposition to model the nonlinear and nonstationary foreign exchange markets. The proposed methodology combines nonparametric kernel regression decomposition with linear (AR and ARIMA) and nonlinear (NPAR and NNAR) forecasting models to separately model long-run trends and short-run fluctuations in exchange rate dynamics. The proposed framework differs from conventional decomposition methods in that it adaptively estimates the underlying trend via local smoothing, without relying on predefined basis functions, frequency-band selection, or iterative mode extraction. Empirical results for five major foreign exchange markets (GBP/USD, EUR/USD, USD/JPY, AUD/USD and USD/CNY) show that the proposed framework consistently outperforms direct hybrid and standalone forecasting models on multiple measures of forecasting accuracy. In addition, the Diebold–Mariano tests show that these improvements are statistically significant and not due to pure random variation. The results also support the proposed symmetry–asymmetry interpretation, implying that by separating relatively symmetric long-run movements from asymmetric short-run fluctuations, forecasting models can more-

efficiently capture the heterogeneous dynamics of foreign exchange markets. Practically, the proposed framework is an interpretable and adaptable forecasting tool for portfolio allocation, hedging, financial risk management, and exchange rate decision-making. The adaptive kernel regression decomposition also makes it easy to extend the framework to other nonlinear and nonstationary financial time series.

Author Contributions: Conceptualization, methodology, and software, H.I.; validation, H.I., S.F.S., F.E.A., and P.C.R.; formal analysis, H.I. and S.F.S.; investigation, H.I. and S.F.S.; resources, F.E.A. and P.C.R.; data curation, H.I. and S.F.S.; writing—original draft preparation, H.I., S.F.S., F.E.A., and P.C.R.; writing—review and editing, H.I., S.F.S., F.E.A., and P.C.R.; visualization, H.I.; supervision, S.F.S.; project administration, S.F.S. and P.C.R.; funding acquisition, F.E.A., and P.C.R. All authors have read and agreed to the published version of the manuscript.

Funding: This work was supported by the Deanship of Scientific Research, Vice Presidency for Graduate Studies and Scientific Research, King Faisal University, Saudi Arabia [Grant No. KFU264452].

Data Availability Statement: The data used in this study were extracted from Yahoo Finance on 25 July 2025.

Conflicts of Interest: The authors declare no conflicts of interest.

References

1. Boyle, P.; McDougall, J. *Trading and Pricing Financial Derivatives: A Guide to Futures, Options, and Swaps*; Walter de Gruyter GmbH & Co. KG: Berlin, Germany, 2018.
2. Jordan, B.D.; Ross, S.A.; Westerfield, R.W. *Fundamentals of Corporate Finance*; McGraw-Hill Irwin: Columbus, OH, USA, 2003.
3. McGuire, P.; von Peter, G.; Zhu, S. International finance through the lens of BIS statistics: The global reach of currencies. *BIS Q. Rev.* **2024**, 1–16. Available online: https://www.bis.org/publ/qtrpdf/r_qt2406b.pdf (accessed on 25 July 2025).
4. Sayari, K.; Ben Belgacem, M. Cryptocurrency and Financial Sector: A Bibliometric Analysis. *Fintech Sustain. Innov.* **2025**, *1*, A8. [CrossRef]
5. Chen, Q. Stock Price Prediction with LLM-Guided Market Movement Signals and Transformer Model. *Fintech Sustain. Innov.* **2025**, *1*, A12. [CrossRef]
6. Khan, F.; Iftikhar, H.; Khan, I.; Rodrigues, P.C.; Alharbi, A.A.; Allohibi, J. A hybrid vector autoregressive model for accurate macroeconomic forecasting: An application to the US economy. *Mathematics* **2025**, *13*, 1706. [CrossRef]
7. Iftikhar, H.; Qureshi, M.; Rodrigues, P.C.; Iftikhar, M.U.; López-Gonzales, J.L. Daily crude oil prices forecasting using a novel hybrid time series technique. *IEEE Access* **2025**, *13*, 98822–98836. [CrossRef]
8. Caporin, M.; Rodríguez Caballero, C.V.; Ruiz Ortega, E. The factor structure of exchange rates volatility: Global and intermittent factors. *Empir. Econ.* **2024**, *67*, 31–45. [CrossRef]
9. Yu, F.; Wang, Y. Empirical Study of Portfolio Rebalancing Strategies in the Chinese ETF Market. *Financ. Res. Lett.* **2026**, *102*, 110119. [CrossRef]
10. Xia, P.; Zhu, X.; Chen, Z.; Jin, F.; He, Q. Predicting Trends in Digital Financial Inclusion: A Novel Approach Based on Spatial Data Analysis and Graph Convolutional Neural Networks. *Comput. Econ.* **2025**, *68*, 2321–2356. [CrossRef]
11. Findlay, J.; McCarthy, R. Developments in Foreign Exchange and Over-the-counter Derivatives Markets. *Bulletin* **2026**. Available online: https://www.rba.gov.au/publications/bulletin/2026/feb/developments-in-foreign-exchange-and-over-the-counter-derivatives-markets.html (accessed on 25 July 2025). [CrossRef]
12. Deng, R.; Xie, H. The Impact of BRICS De-Dollarization on Exchange Rate Fluctuations. *Int. Rev. Econ. Financ.* **2026**, *108*, 105141. [CrossRef]
13. Roy, R.P.; Roy, S.S. Financial contagion and volatility spillover: An exploration into Indian commodity derivative market. *Econ. Model.* **2017**, *67*, 368–380. [CrossRef]
14. Sarno, L.; Taylor, M.P. *The Economics of Exchange Rates*; Cambridge University Press: Cambridge, UK, 2002.
15. Nasr, A.B.; Lux, T.; Ajmi, A.N.; Gupta, R. Forecasting the volatility of the Dow Jones Islamic Stock Market Index: Long memory vs. regime switching. *Int. Rev. Econ. Financ.* **2016**, *45*, 559–571. [CrossRef]
16. Jiang, S.; Yuan, X. Does the e-CNY Pilot Boost Consumption Upgrading? Evidence from China's City-Level Quasi-Experiment. *Appl. Econ. Lett.* **2026**, 1–5. [CrossRef]
17. Sun, X.; Guo, B.; Yang, Y.; Pan, Y. Time for a Change! Uprooting Users Embedded in the Status Quo from Habitual Decision-Making. *Decis. Support Syst.* **2025**, *189*, 114371. [CrossRef]

18. Bank for International Settlements. Triennial Central Bank Survey: Foreign Exchange Turnover in April 2022, 2022. Available online: https://www.bis.org/statistics/rpfx22.htm (accessed on 1 August 2026).
19. Engel, C.; West, K.D. Exchange rates and fundamentals. *J. Political Econ.* **2005**, *113*, 485–517. [CrossRef] [PubMed]
20. Abad, P.; Benito, S.; López, C. A Comprehensive Review of Value at Risk Methodologies. *Span. Rev. Financ. Econ.* **2014**, *12*, 15–32. [CrossRef]
21. Iftikhar, H.; Khan, F.; Rodrigues, P.C.; Alharbi, A.A.; Allohibi, J. Forecasting of inflation based on univariate and multivariate time series models: An empirical application. *Mathematics* **2025**, *13*, 1121. [CrossRef]
22. Diebold, F.X. *Forecasting in Economics, Business, Finance and Beyond*; University of Pennsylvania: Philadelphia, PA, USA, 2017.
23. Gao, K.; Yuan, Y.; Liu, T. Digital Transformation and Value Co-Creation in State-Owned Manufacturing Enterprises: A Hypernetwork Perspective. *Bus. Process. Manag. J.* **2026**, 1–25. [CrossRef]
24. Yule, G.U. On the Time-Correlation Problem, with Especial Reference to the Variate-Difference Correlation Method. *J. R. Stat. Soc.* **1921**, *84*, 497–537. [CrossRef]
25. Wold, H. A Study in the Analysis of Stationary Time Series. Ph.D. Thesis, Almqvist & Wiksell, Uppsala, Sweden, 1938.
26. Box, G.E.P.; Jenkins, G.M.; Reinsel, G.C.; Ljung, G.M. *Time Series Analysis: Forecasting and Control*, 5th ed.; John Wiley & Sons: Hoboken, NJ, USA, 2015.
27. Koopman, S.J.; Ooms, M.; Hindrayanto, I. Periodic Unobserved Cycles in Seasonal Time Series with an Application to US Unemployment. *Oxf. Bull. Econ. Stat.* **2009**, *71*, 683–713. [CrossRef]
28. Ooms, M.; Franses, P.H. A Seasonal Periodic Long Memory Model for Monthly River Flows. *Environ. Model. Softw.* **2001**, *16*, 559–569. [CrossRef]
29. Huo, J. Finite-Difference Solution Ansatz Approach in Least-Squares Monte Carlo. *J. Comput. Financ.* **2025**, *29*, 67–121. [CrossRef]
30. Iftikhar, H.; Khan, M.; Turpo-Chaparro, J.E.; Rodrigues, P.C.; López-Gonzales, J.L. Forecasting stock prices using a novel filtering-combination technique: Application to the Pakistan stock exchange. *AIMS Math.* **2024**, *9*, 3264. [CrossRef]
31. Ren, Y.; Zhang, J.; Xia, Y.; Wang, R.; Xie, F.; Guan, J.; Zhou, S. Regression-Based Conditional Independence Test with Adaptive Kernels. *Artif. Intell.* **2025**, *347*, 104391. [CrossRef]
32. Ghezal, A.; Balegh, M.; Zemmouri, I. Markov-switching threshold stochastic volatility models with regime changes. *AIMS Math.* **2024**, *9*, 3895. [CrossRef]
33. Alzeley, O.; Ghezal, A. On an asymmetric multivariate stochastic difference volatility: Structure and estimation. *AIMS Math.* **2024**, *9*, 18528–18552. [CrossRef]
34. Afuecheta, E.; Okorie, I.E.; Nadarajah, S.; Nzeribe, G.E. Forecasting value at risk and expected shortfall of foreign exchange rate volatility of major African currencies via garch and dynamic conditional correlation analysis. *Comput. Econ.* **2024**, *63*, 271–304. [CrossRef] [PubMed]
35. Poyil, H. Time Series Forecasting Incorporating Exogenous Information. Ph.D. Thesis, KTH Royal Institute of Technology, Stockholm, Sweden, 2019.
36. Tiao, G.C.; Grupe, M.R. Hidden Periodic Autoregressive-Moving Average Models in Time Series Data. *Biometrika* **1980**, *67*, 365–373. [CrossRef]
37. Engle, R.F.; Manganelli, S. CAViaR: Conditional Autoregressive Value at Risk by Regression Quantiles. *J. Bus. Econ. Stat.* **2004**, *22*, 367–381. [CrossRef]
38. Taylor, J.W. Using Exponentially Weighted Quantile Regression to Estimate Value at Risk and Expected Shortfall. *J. Financ. Econom.* **2008**, *6*, 382–406. [CrossRef]
39. Yu, M.; Huang, H.; Hou, R.; Ma, X.; Yuan, S. A Deep Graph Kernel-Based Time Series Classification Algorithm. *Pattern Anal. Appl.* **2024**, *27*, 73. [CrossRef]
40. Li, M.; Li, L.; Zhang, Z.; Zhang, Q. A Novel Method for Generating Permutation Mass Functions Using Permutations to Represent Class Bias. *Expert Syst. Appl.* **2026**, *319*, 132004. [CrossRef]
41. Chen, L.; Pelger, M.; Zhu, J. Deep Learning in Asset Pricing. *Manag. Sci.* **2024**, *70*, 714–750. [CrossRef]
42. Zhou, X.; Zhou, H.; Long, H. Forecasting the Equity Premium: Do Deep Neural Network Models Work? *Mod. Financ.* **2023**, *1*, 1–11. [CrossRef]
43. Shim, J.H.; Kim, Y.S.; Lee, J.W.; Hwang, C. Estimating Value at Risk with Semiparametric Support Vector Quantile Regression. *Comput. Stat.* **2012**, *27*, 685–700. [CrossRef]
44. Sudimanto; Heryadi, Y.; Lukas; Wibowo, A. Foreign Exchange Prediction Using Machine Learning Approach: A Pilot Study. In Proceedings of the 2021 4th International Conference on Information and Communications Technology (ICOIACT), Yogyakarta, Indonesia, 30–31 August 2021; pp. 239–242. [CrossRef]
45. Xu, Q.; Jiang, C.; He, Y. An Exponentially Weighted Quantile Regression via SVM with Application to Estimating Multiperiod VaR. *Stat. Methods Appl.* **2016**, *25*, 285–320. [CrossRef]
46. He, K.; Ji, L.; Tso, G.K.F.; Zhu, B.; Zou, Y. Forecasting Exchange Rate Value at Risk Using Deep Belief Network Ensemble Based Approach. *Procedia Comput. Sci.* **2018**, *139*, 25–32. [CrossRef]

47. Tong, J. Forex-Net: A Hybrid Model for Improved Exchange Rate Prediction Using LSTM and Transfer Learning. *Comput. Econ.* **2026**, *67*, 1413–1427. [CrossRef]
48. Zhou, Y.; Zhu, X. Forecasting USD/RMB exchange rate using the ICEEMDAN-CNN-LSTM model. *J. Forecast.* **2025**, *44*, 200–215. [CrossRef]
49. Tian, H.; Wang, Z.; Zhang, P.; Li, J.; Wang, Q.; Zhang, S. Complex Dynamics of a Symmetric Quantum Stackelberg Duopoly Game Model with Heterogeneous Expectations. *Phys. A Stat. Mech. Appl.* **2026**, *681*, 131073. [CrossRef]
50. Adesina, O.S.; Obokoh, L.O. A hybrid framework of deep learning and traditional time series models for exchange rate prediction. *Sci. Afr.* **2025**, *29*, e02818. [CrossRef]
51. Nasir, J.; Iftikhar, H.; Aamir, M.; Iftikhar, H.; Rodrigues, P.C.; Rehman, M.Z. A Hybrid LMD–ARIMA–Machine learning framework for enhanced forecasting of financial time series: Evidence from the NASDAQ composite index. *Mathematics* **2025**, *13*, 2389. [CrossRef]
52. Iftikhar, H.; Qureshi, M.; Zywiołek, J.; López-Gonzales, J.L.; Albalawi, O. Short-term PM 2.5 forecasting using a unique ensemble technique for proactive environmental management initiatives. *Front. Environ. Sci.* **2024**, *12*, 1442644. [CrossRef]
53. Quispe, F.; Salcedo, E.; Iftikhar, H.; Zafar, A.; Khan, M.; Turpo-Chaparro, J.E.; Rodrigues, P.C.; López-Gonzales, J.L. Multi-step ahead ozone level forecasting using a component-based technique: A case study in Lima, Peru. *AIMS Environ. Sci.* **2024**, *11*, 401–425. [CrossRef]
54. Fan, J.; Yao, Q. *Nonlinear Time Series: Nonparametric and Parametric Methods*; Springer: Berlin/Heidelberg, Germany, 2003.
55. Qureshi, M.; Ishaq, K.; Daniyal, M.; Iftikhar, H.; Rehman, M.Z.; Salar, S.A. Forecasting cardiovascular disease mortality using artificial neural networks in Sindh, Pakistan. *BMC Public Health* **2025**, *25*, 34. [CrossRef] [PubMed]
56. Hyndman, R.J.; Athanasopoulos, G.; Bergmeir, C.; Caceres, G.; Chhay, L.; O'Hara-Wild, M.; Petropoulos, F.; Razbash, S.; Wang, E. Package 'Dorecast'. 2020. Available online: https://cran.r-project.org/web/packages/forecast/forecast.pdf (accessed on 25 July 2025).
57. Di Narzo, A.F.; Aznarte, J.L.; Stigler, M. Package 'tsDyn'. 2013. Available online: http://cran.r-project.org (accessed on 25 July 2025).
58. Hayfield, T.; Racine, J.S. Nonparametric econometrics: The np package. *J. Stat. Softw.* **2008**, *27*, 1–32. [CrossRef]
59. Diebold, F.X. Comparing predictive accuracy, twenty years later: A personal perspective on the use and abuse of Diebold–Mariano tests. *J. Bus. Econ. Stat.* **2015**, *33*, 1. [CrossRef]
60. Iftikhar, H.; Khan, F.; Torres Armas, E.A.; Rodrigues, P.C.; López-Gonzales, J.L. A novel hybrid framework for forecasting stock indices based on the nonlinear time series models. *Comput. Stat.* **2025**, *40*, 4163–4186. [CrossRef]
61. Iftikhar, H.; Zafar, A.; Turpo-Chaparro, J.E.; Canas Rodrigues, P.; López-Gonzales, J.L. Forecasting day-ahead brent crude oil prices using hybrid combinations of time series models. *Mathematics* **2023**, *11*, 3548. [CrossRef]
62. Alraddadi, R. The Markov-switching threshold BLGARCH model. *AIMS Math.* **2025**, *10*, 18838–18860. [CrossRef]
63. Cavicchioli, M.; Ghezal, A.; Zemmouri, I. Bispectral Analysis of Markov Switching Bilinear Models. In *Proceedings of the Scientific Meeting of the Italian Statistical Society*; Springer: Berlin/Heidelberg, Germany, 2024; pp. 373–378.

Disclaimer/Publisher's Note: The statements, opinions and data contained in all publications are solely those of the individual author(s) and contributor(s) and not of MDPI and/or the editor(s). MDPI and/or the editor(s) disclaim responsibility for any injury to people or property resulting from any ideas, methods, instructions or products referred to in the content.